*J. Physiol.* (1975), **251**, *pp.* 1–59
*With* 18 *text-figures*
*Printed in Great Britain*

# RECONSTRUCTION OF THE ELECTRICAL ACTIVITY OF CARDIAC PURKINJE FIBRES

BY R. E. McALLISTER, D. NOBLE AND R. W. TSIEN

*From the Department of Physiology and Biophysics, Dalhousie University, Halifax, N.S., Canada, the University Laboratory of Physiology, Oxford, and the Department of Physiology, Yale University, New Haven, Connecticut 06510, U.S.A.*

(*Received 25 July 1974*)

SUMMARY

1. The electrical activity of cardiac Purkinje fibres was reconstructed using a mathematical model of the membrane current. The individual components of ionic current were described by equations which were based as closely as possible on previous experiments using the voltage clamp technique.

2. Membrane action potentials and pace-maker activity were calculated and compared with time course of underlying changes in two functionally distinct outward currents, $i_{x_1}$ and $i_{K_2}$.

3. The repolarization of the theoretical action potential is triggered by the onset of $i_{x_1}$, which becomes activated over the plateau range of potentials. $i_{K_2}$ also activates during the plateau but does not play a controlling role in the repolarization. However, $i_{K_2}$ does govern the slow pace-maker depolarization through its subsequent deactivation at negative potentials.

4. The individual phases of the calculated action potential and their 'experimental' modifications were compared with published records. The upstroke is generated by a Hodgkin–Huxley type sodium conductance ($g_{Na}$), and rises with a maximum rate of 478 V/sec, somewhat less than experimentally observed values (up to 800 V/sec). The discrepancy is discussed in relation to experimental attempts at measuring $g_{Na}$.

5. The role of the transient outward chloride current (called $i_{qr}$) was studied in calculations of the rapid phase of repolarization and 'notch' configuration. Effects of chloride removal and changes in stimulation rate were simulated by incorporating the effects of these procedures on $i_{qr}$.

6. A secondary inward current partly carried by calcium ions ($i_{si}$) was included in the model and generated a secondary depolarization preceding the plateau. A slowly-rising membrane action potential, based on $i_{si}$, was calculated with $g_{Na} = 0$.

7. The plateau and its dependence on slowly changing currents ($i_{x_1}$ and $i_{si}$) was considered by reconstructing two key phenomena: (*a*) all-or-nothing repolarization under voltage-clamp conditions (Vassalle, 1966) and (*b*) shortening of action potential duration as a result of decreased diastolic interval. The significance of Vassalle's and Weidmann's (1951) observations are reconsidered in light of the results.

8. Membrane currents during simulated voltage clamp steps were calculated using the same formulation which generated the theoretical action potential. Step depolarization to potentials near 0 mV produces a large transient outward chloride current which lasts much longer than the surge of chloride current during the action potential itself. The outward chloride transient overlaps and obscures much smaller changes in $i_{si}$ and $i_{x_1}$ which are, in fact, important to the repolarization of the calculated action potential.

9. The paradoxical effects of subthreshold current pulses on pace-maker activity (Weidmann, 1951) were simulated and could be accounted for by the kinetic properties of $i_{K_2}$.

10. Adrenaline's acceleratory effects on pace-maker activity were reconstructed by incorporating observed voltage-shifts in the kinetic parameters of $i_{K_2}$ under the influence of the hormone.

11. The chronotropic effects of calcium ions were compared with calculations of pace-maker activity which modelled the effects of $[Ca]_o$ on $i_{K_2}$ and $i_{Na}$.

12. The present formulation is based on a mosaic of experimental results and its validity is restricted by limitations in the voltage-clamp technique. It may serve, however, as a framework for studying the interplay of the ionic currents and the effects of their experimental modification on electrical activity.

## INTRODUCTION

In 1952, following their analysis of the ionic currents underlying excitation in squid nerve, Hodgkin & Huxley commented on the possible application of their ideas to other excitable cells: 'The similarity of the effects of changing the concentrations of sodium and potassium on the resting and action potentials of many excitable cells (Hodgkin, 1951) suggests that the basic mechanism of conduction may be the same as implied by our equations, but the great differences in the shape of action potentials show that, even if equations of the same form as ours are applicable in other cases, some at least of the parameters must have very different values.'

During the 1950s relatively little advance was made in obtaining information on the ionic currents in other excitable tissues, such as cardiac and

skeletal muscle, although Frankenhaeuser & Persson (1957) and Dodge & Frankenhaeuser (1958) succeeded in developing a voltage clamp technique for myelinated nerve. The lack of experimental information on a wide variety of tissues prompted several attempts to find simple theoretical modifications of the original H–H equations which would reproduce electrical activity very different from that which normally occurs in squid nerve. These attempts developed almost simultaneously so that within a short period of time all the simple modifications which would give rise to long-lasting action potentials of the kind observed in cardiac muscle had been explored (FitzHugh, 1960; Brady & Woodbury, 1960; Noble, 1960, 1962*a*; George & Johnson, 1961).

In retrospect, these modifications seem surprisingly simple. FitzHugh and George & Johnson slowed the activation of the potassium conductance in order to reproduce the long-lasting action potentials in TEA treated nerve. Noble included the marked inward rectification displayed by the potassium current in cardiac membranes. Brady & Woodbury also included this rectification, but slowed a component of the sodium inactivation process instead of including a slowly activated potassium conductance. Despite their simplicity, these models were very successful in accounting for a wide range of electrical activity.

By 1962, therefore, the theory of long-lasting action potentials had developed much further than the experimental work and it did not seem fruitful to explore further theoretical modifications until quantitative information on the ionic currents became available. Obtaining this information has proved to be a slow process. The voltage, clamp technique was first successfully applied to cardiac membranes about 10 years ago (Deck, Kern & Trautwein, 1964; Hecht, Hutter & Lywood, 1964) but we still do not have a quantitative description of the ionic currents as complete as that provided by Hodgkin & Huxley in the case of squid nerve. The reasons for this slow progress are partly that it is technically difficult to control the membrane potential during the activation of the sodium conductance in cardiac muscle (see, for example, Beeler & Reuter, 1970; New & Trautwein, 1972; Johnson & Lieberman 1971), and partly that the number of components of ionic current responsible for electrical activity is much greater than in nerve (see also Trautwein, 1973; Noble, 1974).

However, sufficient experimental information has now accumulated to show that all the early modifications of the H–H equations are inadequate in important ways. Although we cannot formulate a model as accurate as that given by Hodgkin & Huxley, we may, nevertheless, correct many of these inadequacies by basing new ionic current equations on as much of the experimental information as possible. The model we have constructed will be useful, we believe, partly because it forms a quantitative summary of

our present state of knowledge, partly because it can be used to give accounts or explanations of a wide range of electrical behaviour in Purkinje fibres and, finally, because it indicates some areas where further experiments would be worth while.

We should, nevertheless, emphasize the limitations of the present paper. Firstly, we shall be concerned solely with membrane (or uniform) action potentials. We have not used the model to reproduce conduction and there may be serious difficulties in doing so at this stage (see Discussion). Secondly, since it is impossible to obtain experimental information on all the current mechanisms from a single preparation, we must rely on collecting the information from different preparations. The model is therefore a mosaic of various experimental results and one of our aims has been to see how the results on different current components from different preparations may be matched to produce a working model. Finally, and most importantly, the voltage clamp data are still incomplete or inadequate in certain respects. Where this is so, we have been guided to some extent by the known action potential characteristics so that the predictive value of the model is necessarily restricted. Our justification for proceeding to construct a model despite some incompleteness is that it seems likely that we are close to the limit of what experimental information can be obtained on the kinetics and magnitudes of the current components using present techniques. This information is already sufficiently complex to require a useful quantitative summary.

Some of this work has been previously reported in abstract form (Hauswirth, McAllister, Noble & Tsien, 1968, 1969).

## DESCRIPTION OF CURRENT COMPONENTS

### *Capacity current*

The low-frequency capacitance of Purkinje fibres is about 12 $\mu$F/cm$^2$ when referred to the cylindrical surface area of the bundle of cells (Weidmann, 1952). This value is much larger than that for nerve membranes, which have a capacitance of about 1 $\mu$F/cm$^2$. It is now fairly certain that this large difference arises because the cylindrical surface area is only a small fraction of the total cell membrane area. Mobley & Page (1972) have shown that a large fraction of the cell membrane lies deep in the bundle where the cells are separated by narrow clefts (see also Sommer & Johnson, 1968). When membrane folding is also taken into account, the true membrane area is about 10 times larger than the cylindrical surface area and the true membrane capacitance is about 1 $\mu$F/cm$^2$. Most of the ionic current data from voltage clamp experiments are nevertheless referred to the cylindrical surface area of the bundles. The appropriate value of the

capacitance to be charged or discharged by the ionic currents is therefore about 10 $\mu$F/cm$^2$. We shall use this value throughout the present paper. An alternative approach would be to divide all ionic currents by a factor of 10 and refer the currents and capacitance to unit area of cell membrane. This would produce the same results in the case of uniform action potentials.

The more substantial assumption implicit in this approach is that the capacitance and the various ionic currents have the same cross-sectional distribution in the deep and surface membranes of a bundle, i.e. the ionic current densities are uniform throughout the bundle. Provided that this is the case, the presence of a significant cleft resistance will not influence the currents and voltage changes in a strictly 'uniform' action potential since there are then no extracellular or intracellular gradients. The problems that arise when these assumptions are incorrect will be discussed later (see Discussion).

That the capacitance and the various ionic currents should be similarly distributed throughout the preparation is itself a condition for strictly uniform action potentials to be possible. Thus, if the surface and cleft membranes differ in their abilities to generate sodium current, one area of membrane will become depolarized faster than the other, and non-uniformities will then appear.

The equation for a uniform response is well known:

$$\frac{dE}{dt} = -\frac{i_1}{C}, \tag{1}$$

where $E$ is membrane potential (mV), $t$ is time (msec), $i_1$ is the sum of the ionic currents flowing across the membrane ($\mu$A/cm$^2$) and $C$ is the membrane capacitance ($\mu$F/cm$^2$).

### *General comments on ionic current components*

In the following section, we consider the various components of ionic current revealed by previous studies, and their quantitative description in the model. Although the number of components is larger than in some other excitable membranes (e.g. squid nerve) their incorporation seems justified, both from the experimental results, and because each of the components appears to play at least some role in the range of activity exhibited by Purkinje fibres. An obvious question is whether each of the components corresponds to a genuine and distinct permeability process (Johnson & Lieberman, 1971). Although the answer is uncertain, the available evidence suggests that the components are at least functionally distinct (see Hauswirth, Noble & Tsien, 1972*b*). Studies of ionic composition,

gating kinetics, and sensitivity to pharmacological agents provide considerable support for this distinction.

In place of the single sodium current in squid nerve there are two time-dependent inward currents. The first, $i_{Na}$, resembles the squid sodium current. The second, $i_{si}$, has slower kinetics and is at least partly carried by calcium ions.

Unlike squid, the chloride current in the Purkinje fibre shows dynamic behaviour in the form of a transient outward current, $i_{qr}$, activated during strong depolarizations.

In place of the single potassium current we find three distinguishable time-dependent potassium currents, $i_{K_2}$, $i_{x_1}$ and $i_{x_2}$, none of which resembles the squid potassium current from a quantitative point of view.

In describing the kinetics of these current components, we have retained the formalism of the Hodgkin–Huxley equations. The experimentally observable time-dependence is attributed to gating reactions, described by Hodgkin–Huxley-type variables ($m$, $h$, $s$ and so forth). These variables range between zero and one and each obey the usual first order equation

$$\frac{dy}{dt} = \alpha_y(1-y) - \beta_y(y), \quad \text{where} \quad y = m, h, s, \text{ etc.} \tag{2}$$

Differences between the kinetic behaviour of one component and another are thus reflected in the individual rate coefficients (see Table 1).

The outward potassium currents change exponentially with step changes in membrane potential. In their case, the actual current at any moment is very simply related to the gating variable by the general expression:

$$i = y\,\bar{\imath}, \quad \text{where} \quad y = s, x_1 \text{ or } x_2. \tag{3}$$

Here $\bar{\imath}$ is a 'fully-activated current–voltage relationship' which describes the characteristics of the component when all its channels are open ($y = 1$). $\bar{\imath}$ is a linear function of potential in some cases,

$$\bar{\imath} = \bar{g}(E - E_{rev}), \quad \text{where } g \text{ is a constant} \tag{4}$$

but in other cases, a non-linear function was used (see p. 16 below).

Unlike the potassium currents, $i_{Na}$, $i_{si}$ and $i_{qr}$ show inactivation following step depolarizations (see Reuter, 1968). These components are each turned on by depolarizations into the plateau range of potentials, but maintained depolarizations lead to a decline in conductance. To describe this phasic behaviour, we followed Hodgkin & Huxley (1952) in using two gating variables, one for activation, and another for inactivation. For example, the transient chloride current $i_{qr}$ is described as follows:

$$i_{qr} = q.r.\bar{\imath}_{qr}, \quad \text{where} \quad \bar{\imath}_{qr} = \bar{g}_{qr}(E - E_{Cl}). \tag{5}$$

The inactivation variable ($r$ in this case) has rate coefficients ($\alpha_r$ and $\beta_r$, see Table 1) which cause the variable to decline as the membrane potential becomes less negative.

TABLE 1*A*

| Component | $\alpha$ | $\beta$ | $\bar{\alpha}$ (msec$^{-1}$) | $\bar{\beta}$ (msec$^{-1}$) | $\bar{E}$ (mV) | $\bar{g}$ (mmho/cm$^2$) | $E_{rev}$ (mV) |
|---|---|---|---|---|---|---|---|
| Current components which show inactivation | | | | | | | |
| $i_{Na}$ | $\alpha_m = \dfrac{\bar{\alpha}_m(E-\bar{E}_m)}{1-\exp-\dfrac{(E-\bar{E}_m)}{10}}$ | $\beta_m = \bar{\beta}_m \exp-\dfrac{(E-\bar{E}_m)}{17{\cdot}86}$ | 1·0 | 9·86 | −47 | 150 | +40 |
| | $\alpha_h = \bar{\alpha}_h \exp-\dfrac{(E-\bar{E}_h)}{5{\cdot}43}$ | $\beta_h = \bar{\beta}_h\left[1+\exp-\dfrac{(E-\bar{E}_h)}{12{\cdot}2}\right]^{-1}$ | $1{\cdot}13\times10^{-7}$ | 2·5 | −10 | | |
| $i_{si}$ | $\alpha_d = \dfrac{\bar{\alpha}_d(E-\bar{E}_d)}{1-\exp-\dfrac{(E-\bar{E}_d)}{10}}$ | $\beta_d = \bar{\beta}_d \exp-\dfrac{(E-\bar{E}_d)}{11{\cdot}26}$ | 0·002 | 0·02 | −40 | 0·8 | +70 |
| | $\alpha_f = \bar{\alpha}_f \exp-\dfrac{(E-\bar{E}_f)}{25}$ | $\beta_f = \bar{\beta}_f\left[1+\exp-\dfrac{(E-\bar{E}_f)}{11{\cdot}49}\right]^{-1}$ | 0·00253 | 0·02 | −26 | | |
| $i_{qr}$ | $\alpha_q = \dfrac{\bar{\alpha}_q(E-\bar{E}_q)}{1-\exp-\dfrac{E-\bar{E}_g}{10}}$ | $\beta_q = \bar{\beta}_q \exp-\dfrac{(E-\bar{E}_q)}{11{\cdot}26}$ | 0·008 | 0·08 | 0 | 2·5 | −70 |
| | $\alpha_r = \bar{\alpha}_r \exp-\dfrac{(E-\bar{E}_r)}{25}$ | $\beta_r = \bar{\beta}_r\left[1+\exp-\dfrac{(E-\bar{E}_r)}{11{\cdot}49}\right]^{-1}$ | $2{\cdot}08\times10^{-5}$ | 0·02 | −26 | | |
| | $\alpha'_r = \bar{\beta}'_r \exp-\dfrac{(E-E'_r)}{17}$ | $\beta'_r = \bar{\beta}'_r\left[1+\exp-\dfrac{(E-\bar{E}'_r)}{8}\right]^{-1}$ | $1{\cdot}93\times10^{-4}$ | 0·033 | −30 | | |

Each component is controlled by a pair of gating variables. In each case, the rate coefficients for the activation variable are described in the upper row, and those of the inactivation variable in the lower row. The $\alpha$s and $\beta$s are given in a form to allow direct comparison with expressions for skeletal muscle and squid nerve (Adrian, Chandler & Hodgkin, 1970, Table 6). $E$ is membrane voltage in the sense of inside potential minus outside potential. Fully activated current–voltage relationships are given by $\bar{\imath} = \bar{g}(E-E_{rev})$, where $\bar{g}$ and $E_{rev}$ are indicated in the two right-hand columns. $\alpha'_r$ and $\beta'_r$ are from Fozzard & Hiraoka (1973).

TABLE 1*B*

| Component | $\alpha$ | $\beta$ | $\bar{\alpha}$ (msec$^{-1}$) | $\bar{\beta}$ (msec$^{-1}$) | $\bar{E}$ (mV) | $\bar{g}$ (mmho/cm$^2$) | $E_{rev}$ (mV) |
|---|---|---|---|---|---|---|---|
| | | Slow outward K currents | | | | | |
| $i_{K_2}$ | $\alpha_s = \dfrac{\bar{\alpha}_s(E-\bar{E}_s)}{1-\exp-\dfrac{(E-\bar{E}_s)}{5}}$ | $\beta_s = \bar{\beta}_s \exp-\dfrac{(E-\bar{E}_s)}{14{\cdot}93}$ | 0·001 | $5{\cdot}0\times10^{-5}$ | −52 | (rectifying) | −110 |
| $i_{x_1}$ | $\alpha_{x_1} = \dfrac{\bar{\alpha}_{x_1}\exp\dfrac{E+50}{12{\cdot}1}}{1+\exp\dfrac{E+50}{17{\cdot}5}}$ | $B_{x_1} = \dfrac{\bar{\beta}_{x_1}\exp-\dfrac{E+20}{16{\cdot}67}}{1+\exp-\dfrac{E+20}{25}}$ | $5\times10^{-4}$ | 0·0013 | — | (rectifying) | −95 |
| $i_{x_2}$ | $\alpha_{x_2} = \bar{\alpha}_{x_2}\left[1+\exp-\dfrac{E+19}{5}\right]^{-1}$ | $\beta_{x_2} = \dfrac{\bar{\beta}_{x_2}\exp-\dfrac{E+20}{16{\cdot}67}}{1+\exp-\dfrac{E+20}{25}}$ | $1{\cdot}27\times10^{-4}$ | $3\times10^{-4}$ | — | 0·385 | −65 |

Each component is controlled by a single activation variable, with corresponding rate coefficients as tabulated. No value of $\bar{E}$ is entered for $x_1$ or $x_2$, because no common voltage parameter could be used for $\alpha$ and $\beta$ in these cases.The fully activated current–voltage relationships of $i_{K_2}$ and $i_{x_1}$ show inward-going rectification (see text).

Further explanation and justification for the framework for describing the components is given in Noble (1972*a*) and Noble & Tsien (1968). We now proceed with the description of the individual ionic currents.

*Excitatory sodium current, $i_{Na}$*

This current component strongly resembles the sodium current in squid nerve. It is specifically blocked by tetrodotoxin (Dudel, Peper, Rüdel & Trautwein, 1967*b*). It is also clear that, as in nerve, the sodium current may be described in terms of the two gating variables, $m$ and $h$ (Dudel & Rüdel, 1970). However, it has not proved possible to accurately measure the magnitude or kinetics of $i_{Na}$ in Purkinje fibres under normal physiological conditions. In most preparations the sodium current is too large to allow adequate voltage clamping using high-resistance micro-electrodes. Moreover, since the decay of capacitance current requires several milliseconds (Fozzard, 1966; Freygang & Trautwein, 1970), the time course of onset of $i_{Na}$ is initially obscured by the decay of $i_c$.

Dudel & Rüdel (1970) partly overcame this difficulty by analysing the sodium current at low temperature (8° C), when the time course is slowed by a factor of about 30. In those fibres in which $i_{Na}$ was not so large as make clamping clearly impossible, they were able to successfully analyse the time course of $i_{Na}$. Their overall conclusion that the kinetics resemble the $m$ and $h$ kinetics of squid nerve will be used as the main experimental justification for using these kinetics in our model. Unfortunately, though interestingly, Dudel & Rüdel's results show that the effect of temperature on the $h$ kinetics is not simply equivalent to applying a scaling factor to the time axis. Thus, the steady-state inactivation curve, $h_\infty(E)$ is shifted strongly in the hyperpolarizing direction by cooling. Below 20° C the shape of the curve is also changed. It is not therefore possible to apply a simple $Q_{10}$ factor to extrapolate from Dudel & Rüdel's results to the kinetics of the sodium current at normal (*ca.* 37° C) temperatures. Nevertheless, the results do allow approximate extrapolations to be made and these indicate that at normal temperatures the sodium current activates with a time constant of about 0·1 msec and should be fully inactivated within a millisecond or so. These time constants are very similar to those obtained on nerve fibres, despite the fact that the nerve results were obtained at lower temperatures than 37° C.

These conclusions also confirm Weidmann's (1955*a*) analysis of the sodium current inactivation kinetics in Purkinje fibres. He used a method for determining the $h$ kinetics without using full voltage clamp techniques and found that the $h$ kinetics strongly resemble those for nerve, although the $h_\infty(E)$ curve obtained was rather steeper than that obtained by Hodgkin & Huxley (1952). In view of the uncertainties involved in

applying the voltage clamp technique to $i_{Na}$ in Purkinje fibres, we think that Weidmann's data are still the best available on $h$ and we shall therefore use the equations:

$$\alpha_h = 0{\cdot}0085 \exp[-0{\cdot}184(E+71)], \tag{5}$$

$$\beta_h = 2{\cdot}5/(\exp[-0{\cdot}082(E+10)]+1). \tag{6}$$

These expressions fit his data (cf. Noble 1962*a*) when allowance is made (Weidmann, 1955*b*) for the $[Ca]_o$ in his experiments (2·6 mM instead of the 'standard' concentration of 1·8 mM).

For the $m$ kinetics, we shall use the equations given by Hodgkin & Huxley (1952). We shall set the voltage dependence to give a similar separation between $E(m_\infty = 0{\cdot}5)$ and $E(h_\infty = 0{\cdot}5)$, which is about 24 mV in squid nerve. For the Purkinje fibre this requires $m_\infty = 0{\cdot}5$ at $E_m = -47$ mV. This is close to the value of about $-45$ mV for this point given by Dudel & Rüdel's (1970, Fig. 4) results at low temperatures. The equations for $m$ are then:

$$\alpha_m = (E+47)/(1-\exp[-0{\cdot}1(E+47)]), \tag{7}$$

$$\beta_m = 40 \exp[-0{\cdot}056(E+72)] \tag{8}$$

and for $i_{Na}$:

$$i_{Na} = \overline{i_{Na}}.m^3.h, \tag{9}$$

$$\overline{i_{Na}} = \overline{g_{Na}}.(E-E_{Na}). \tag{10}$$

It remains to assign values to $E_{Na}$ and $\overline{g_{Na}}$. The low temperature results of Dudel & Rüdel are, again, difficult to use since $E_{Na}$ clearly falls as the fibres are cooled. Soon after cooling to 8° C, Dudel & Rüdel obtained +30 mV. Later, this value fell to 0 (as expected if the sodium pump ceases to operate at low temperatures). Their results are therefore consistent with the normal value of $E_{Na}$ being larger than +30 mV. Draper & Weidmann (1951) obtained a value of about +40 to +50 mV for the peak of the action potential, which they showed to obey the Nernst relation for a sodium permeable membrane. The value we have chosen to use in the model is +40 mV.

The value of $\overline{g_{Na}}$ remains very uncertain. Since a substantial number of Purkinje fibre preparations do not allow the sodium current to be clamped without inducing oscillations, it is fairly certain that *all* the voltage clamp estimates must be lower than average since they are obtained on fibres in which the current is small enough for effective clamping. Moreover, it is unlikely that the voltage clamp technique records all the sodium current even in these preparations since the development of non-uniformity in the clefts of the preparation (Johnson & Lieberman, 1971) will ensure that some of the sodium current that may flow in the clefts will not be recorded. Since the cleft membranes account for 90 % of the total membrane area

(Mobley & Page, 1972), the fraction of unrecorded sodium current may be very substantial.

In the light of these considerations, it is interesting to note that the voltage clamp estimates of $\overline{g_{Na}}$ in Purkinje fibres are indeed very much smaller than in other tissues. For example, Dudel & Rüdel estimate a value of 53 mmho/cm$^2$ referred to the surface area of the preparation which they compare with 20–90 mmho/cm$^2$ in squid nerve. However, if this sodium conductance were uniformly distributed in the cleft and surface membranes, the true value would be as low as 5·3 mmho/cm$^2$ which is only a small fraction of that obtained in squid.

By contrast, estimates of $\overline{g_{Na}}$ that do not require the voltage clamp technique indicate that it is comparable to that in squid. The maximum rate of depolarization attained during the action potential is about 600–800 V/sec which is similar to rates observed in nerve action potentials. Moreover, by assuming the sodium current density to be the same as in squid, it is possible to calculate values for the liminal length for excitation (Noble 1972*b*) within the range of experimental values obtained by Fozzard & Schoenberg (1972). A tenfold lower sodium current would increase the liminal length by a factor of about 3 (the liminal length is inversely proportional to the square root of the excitatory current density near threshold, Noble, 1972*b*, eqn. (12)) which would be well outside Fozzard & Schoenberg's experimental range of values.

It appears, therefore, that the lower limit for $\overline{g_{Na}}$ must be considerably larger than 50 mmho/cm$^2$ referred to surface area of preparation (or 5 mmho/cm$^2$ referred to true membrane area).

An upper limit is, in practice, set by experimental knowledge of membrane current–voltage relations at times when the sodium current approximates to steady-state values. In particular, the magnitude of the steady-state sodium current in the model must not be large enough to prevent the onset of outward currents from abolishing the net inward current regions of these current–voltage relations. Otherwise repolarization will not occur following excitation.

During slow phases of activity, such as the plateau of the action potential, the kinetic variables will be rather close to their steady-state values, $m_\infty$ and $h_\infty$, so that the sodium system will contribute approximately

$$(i_{Na})_\infty = \overline{g_{Na}}(E - E_{Na})m^3{}_\infty h_\infty. \tag{11}$$

For a range of potentials near threshold both the $m_\infty$ and $h_\infty$ variables have significantly large values and $|(i_{Na})_\infty|$ approaches a maximum, i.e. the $(i_{Na})_\infty$ *vs.* $E_m$ relation shows a rounded hump (see curve *b* in Fig. 2). The amplitude of this hump will contribute to determining the difference

between the peak and trough of the overall current–voltage relationship during the slow phases of electrical activity (see Fig. 3). As we shall show later, our estimates of the amplitudes of the other current components contributing to the $i_1(E)$ relations leave an upper bound for the value of $(i_{Na})_\infty$ which is about 4 $\mu$A/cm$^2$. A suitable choice for $\overline{g_{Na}}$ which keeps $(i_{Na})_\infty$ within this maximum and which is considerably larger than the voltage clamp estimates of $\overline{g_{Na}}$ is 150 mmho/cm$^2$. Taking Mobley & Page's membrane area estimates into account, this value corresponds to a value of 15 mmho/cm$^2$ when referred to total membrane area. This is rather smaller than the lowest values for squid nerve and would produce liminal length estimates just within the experimental range of values given by Fozzard & Schoenberg.

It should be noted that there are necessarily some interrelations between the sodium conductance parameters chosen. In particular the maximum value of $(i_{Na})_\infty$ is very sensitive to the steepness and degree of overlap of the $m_\infty$ and $h_\infty$ curves. One consequence of using Weidmann's steeper $h_\infty(E)$ relation is that the peak value of $(i_{Na})_\infty$ is reduced so that there is a relatively large ratio between the peak transient current occurring during the action potential upstroke and the steady-state current. An increase in the degree of overlap between $m_\infty(E)$ and $h_\infty(E)$, or a decrease in the steepness of either of these relations would greatly increase the relative value of $(i_{Na})_\infty$ and so reduce the value of $\overline{g_{Na}}$ required to produce a given value of $(i_{Na})_\infty$. This value is also sensitive to the shape of the $h_\infty$ and $m_\infty$ curves at small values ($< 0{\cdot}1$) for which there is very little experimental information, even for squid nerve (Hodgkin & Huxley, 1952).

A related problem is the location of the sodium threshold in relation to the position of the $m_\infty(E)$ curve. The choice of this position might appear to be important in determining the absolute level of the excitatory threshold. In fact, it is less crucial because of the constraint on the peak steady-state sodium current. Shifting $m_\infty(E)$ in the depolarizing direction decreases the $m$-$h$ overlap and allows $\overline{g_{Na}}$ to be increased. These two procedures largely balance in their effect on the threshold for uniform excitation.

*The secondary inward current, $i_{si}$*

This component has been referred to as 'secondary' (Johnson & Lieberman 1971) because its time course is considerably slower than that of the 'primary' sodium current $i_{Na}$. Other authors have used the name 'slow inward current'. The term 'secondary' may be more appropriate: the time course of $i_{si}$ is certainly slow in relation to $i_{Na}$, but not in comparison to the plateau outward currents $i_{x_1}$ and $i_{x_2}$.

The voltage clamp results of various authors are quite consistent in their description of $i_{si}$ and we have relied upon published records in formulating the model. It should be pointed out, however, that interpretations of the voltage clamp results may be somewhat confusing; Reuter (1968) refers to $i_{si}$ as 'slow sodium inactivation' while Peper & Trautwein (1968) have called it the 'negative dynamic current'. The

dynamic current hypothesis will be considered in a later section. In formulating the model we have accepted Vitek & Trautwein's (1971) evidence that the 'negative dynamic current' and the 'positive dynamic current' are, in fact, two genuinely distinct components, namely $i_{s1}$ and $i_{qr}$ (see also Trautwein, 1973).

$i_{s1}$ has been distinguished from $i_{Na}$ by its pharmacological sensitivity as well as its kinetics (see Reuter, 1973). It is typically activated by a step depolarization from $-80$ to potentials positive to about $-50$ mV: the threshold lies beyond that for $i_{Na}$. The inward current reaches a peak in 5–10 msec (Vitek & Trautwein, 1971) and then declines, roughly exponentially, with a time constant of about 50 msec. The inward current decline is quite often masked by the appearance of the outward chloride transient $i_{qr}$ (cf. Peper & Trautwein, 1968). In these cases, the time course of $i_{s1}$ may nevertheless be obtained indirectly, by studying the inward transients *following* repolarization, as a function of the duration of the previous depolarization. The envelope of the inward current tails indicates the time course of $i_{s1}$ inactivation. Use of this technique (e.g. Reuter, 1968, Fig. 4) supports the finding that $i_{s1}$ inactivation proceeds with a time constant of about 50 msec in the plateau range of potentials.

The instantaneous current voltage relation of $i_{s1}$ was studied by Vitek & Trautwein (1971). These authors found a linear I–V relation, extrapolating to a reversal potential ranging between $+40$ and $+60$ mV. The relatively positive level of the apparent reversal potential is consistent with the results of ion replacement experiments which suggest that both Ca and Na ions may contribute to the secondary inward current (Vitek & Trautwein, 1971; cf. Rougier, Vassort, Garnier, Gargouil & Coraboeuf, 1969). In the reconstruction we have used the expression

$$\overline{i_{s1}} = \overline{g_{s1}}(E - E_{s1}), \tag{12}$$

where $E_{s1} = +70$ mV and where $\overline{g_{s1}}$ was usually assigned the value 0·8 mmhos/cm$^2$. It should be noted that the reconstructed plateau is not critically dependent on the value chosen for $E_{s1}$, but rather on the magnitude of $\overline{i_{s1}}$ in the plateau range of potentials.

The activation process is not well described in Purkinje fibres. We have assumed that activation is governed by a variable $d$, raised to the first power (see Reuter, 1973). The rate constants for $d$ are identical in form to the sodium activation variable, $m$, but are slowed so that $\tau_d = 12$ msec at 0 mV. $d_\infty = 0{\cdot}5$ at $-40$ mV, in conformity with Reuter's activation curve (1968, Fig. 2), but considerably more negative in location than Vitek & Trautwein's curve, which is half-maximal at approximately $-20$ mV. It seems possible therefore that there is some variation between fibres in the position of the $d_\infty(E)$ curve.

The process of inactivation is quite important to the behaviour of the model action potential. Reuter (1968, Fig. 4) suggests that a sizable fraction of $i_{si}$ (ranging from one fifth to one half) may not be inactivated, even during prolonged depolarizations to the plateau range. The immediate consequence of this incomplete inactivation is that residual $i_{si}$ will contribute to a region of net inward current in the plateau range. According to the analysis of Noble & Tsien (1969*b*) this inward current would maintain the plateau indefinitely, were it not for the activation of $i_{x_1}$ (see p. 35).

We have chosen to express the existence of residual $i_{si}$ by the following expression:

$$i_{si} = \overline{g_{si}}(E-E_{si}).d.f+\overline{g'_{si}}(E-E_{si}).d'. \tag{13}$$

In the calculations, unless otherwise stated, $\overline{g_{si}} = 0{\cdot}8$ mmho/cm$^2$, $\overline{g'_{si}} = 0{\cdot}04$ mmho/cm$^2$, and $E_{si} = +70$ mV. These parameter values give a residual $i_{si}$ of roughly 6 $\mu$A/cm$^2$ at $-40$ mV (see curve *c* in Fig. 2). Eq. (14) may be given the physical interpretation that a certain fraction of the channels (maximum conductance $\overline{g'_{si}}$) simply lack the property of inactivation. Presumably channels do show activation – the variable $d'$ is similar or perhaps identical to $d$. The results in this paper were calculated with a time-independent expression for $d'$, which nearly coincides with $d_\infty$:

$$d' = (1+\exp(-0{\cdot}15(E+40)))^{-1}. \tag{13a}$$

Another possibility is to set $d' = d$. This prolongs the calculated action potential by about 50 msec but otherwise gives similar results. A third possibility (R. H. Brown & D. Noble, unpublished) is to attribute the existence of appreciable steady-state $i_{si}$ to a significant overlap of the $d$ and $f$ processes. This formulation is appealing because it uses the simpler equation (12); the steady-state current is thus $\bar{g}_{si}(E-E_{si})d_\infty f_\infty$ (the overlap between $d_\infty$ and $f_\infty$ in ventricular muscle is substantial and at $-25$ mV as much as 15 % of the maximum conductance would remain activated in the steady state (see Reuter, 1973, Fig. 6)). Each of these formalisms expresses the presence of residual secondary inward current, and gives a reasonable action potential reconstruction. The final choice between various expressions will depend upon better experimental information.

The equations used for the rate constants are

$$\alpha_d = 0{\cdot}002(E+40)/(1-\exp[-0{\cdot}1(E+40)]), \tag{14}$$

$$\beta_d = 0{\cdot}02\exp[-0{\cdot}0888(E+40)], \tag{15}$$

$$\alpha_f = 0{\cdot}000987\exp[-0{\cdot}04(E+60)], \tag{16}$$

$$\beta_f = 0{\cdot}02/(\exp[-0{\cdot}087(E+26)]+1), \tag{17}$$

which reproduce the experimental values of the speeds of activation and inactivation in the plateau range of potentials.

*Note on terminology for outward current components*

The voltage clamp analysis of the kinetics of the outward current components is fairly complete and, by contrast with the inward currents, there is little difficulty in assigning appropriate equations to describe them. The terminology used is, however, somewhat confusing and it may help if we briefly explain the terminology we shall employ.

The earliest experiments on the voltage dependence of the Purkinje fibre potassium current demonstrated the existence of both time-independent and time-dependent components (Hutter & Noble 1960; Hall, Hutter & Noble, 1963). It was therefore natural to refer to these two components as $i_{K_1}$ and $i_{K_2}$ respectively and this was the terminology used by Noble (1962*a*). The time-independent component was found to be highly non-linear, $g_{K_1}$ being greatly reduced by depolarization (Hutter & Noble, 1960; Carmeliet, 1961; Hall *et al.* 1963; Deck & Trautwein, 1964). The time-dependent component was modelled by a conductance mechanism of the Hodgkin–Huxley type which begins to turn on at about $-40$ mV.

The early voltage clamp experiments confirmed the existence of time-independent and time-dependent components (McAllister & Noble, 1966) but the component first identified as time-dependent, and therefore called $i_{K_2}$, was later found to have a very negative threshold at about $-90$ mV (Noble & Tsien, 1968). Subsequent work resolved this problem by demonstrating the existence of a second voltage range (at plateau potentials) in which time-dependent potassium currents could be recorded (Noble & Tsien, 1969*a*). Although these currents were clearly those responsible for the time-dependent changes seen by Hall *et al.* (1963), it would have been confusing to call these currents $i_{K_2}$. Moreover, since it was found (Noble & Tsien, 1969*a*) that the mechanisms responsible for the plateau outward currents were less selective to potassium ions than the component $i_{K_2}$ identified by Noble & Tsien (1968) it was decided that the symbol $i_x$ would be appropriate to emphasize the presence of small contributions from ions other than potassium. Since $i_x$ was found to be separable into two first-order mechanism with easily distinguishable kinetics, the terms $i_{x_1}$ and $i_{x_2}$ were introduced to describe the fast and slow components respectively of $i_x$.

A more detailed discussion of the problems of terminology and identification of potassium current components will be found in Noble & Tsien (1969*a*, *b*). We shall first describe the equations we shall use for the time-dependent components, $i_{K_2}$, $i_{x_1}$, and $i_{x_2}$. The time-independent component will be described later (see 'Background current components').

*The pacemaker potassium current, $i_{K_2}$*

The component $i_{K_2}$ is activated over the 'pace-maker' range of potentials. The gating variable $s_\infty$ is 0 at about $-90$ mV and approaches 1 at about $-60$ mV. Since this current controls pacemaker activity we shall also refer to it as the pace-maker potassium current. The general equation is

$$i_{K_2} = \overline{i_{K_2}} \cdot s, \tag{18}$$

where $\overline{i_{K_2}}$ describes the fully activated current–voltage relation and $s$ follows first order kinetics described by eqn. (2) with rate coefficients:

$$\alpha_s = 0{\cdot}001(E+52)/(1-\exp[-0{\cdot}2(E+52)]), \tag{19}$$

$$\beta_s = 0{\cdot}00005 \exp[-0{\cdot}067(E+52)]. \tag{20}$$

These equations fit the experimental values for $\alpha_s$ and $\beta_s$ given by Noble & Tsien (1968, Fig. 4).

The ion transfer described by the fully activated current flow, $\overline{i_{K_2}}$, is a highly non-linear process. The relation in the vicinity of $E_K$ (about $-100$ mV for $[K]_0 = 4$ mM or $-115$ mV for $[K]_0 = 2$ mM) was obtained by Noble & Tsien (1968, Figs. 8, 9). Their results show that this relation shows marked inward-going rectification with a negative slope conductance appearing at voltages more than 20–30 mV positive to $E_K$. Hauswirth *et al.* (1972*b*) have shown that this negative slope conductance persists at strong depolarizations so that $\overline{i_{K_2}}$ tends towards zero at about 0 mV.

The mechanism of inward-going rectification is not yet clear, but Adrian (1969) has described a relatively simple charged carrier model that reproduces current–voltage relations like that for $\overline{i_{K_2}}$. We shall therefore use his function (Adrian, 1969, eqn. 15.1) to describe $\overline{i_{K_2}}$. For our case the appropriate equation is

$$\overline{i_{K_2}} = 2{\cdot}8(\exp[0{\cdot}04(E+110)]-1)/(\exp[0{\cdot}08(E+60)]+\exp[0{\cdot}04(E+60)]). \tag{21}$$

The reversal potential has been assumed to lie at $E_K$ as shown by the results of Noble & Tsien (1968) and Peper & Trautwein (1969). In 2·7 mM-$[K]_0$, $E_K$ is taken as $-110$ mV. Eqn. (23) is plotted in Fig. 1 together with the $\bar{i}$ functions for the other potassium current components. This curve effectively reproduces the experimental relations obtained by Noble & Tsien (1968) and by Hauswirth *et al.* (1972*b*).

*The 'plateau' potassium currents, $i_{x_1}$ and $i_{x_2}$*

The equations we shall use for these currents are based on the experimental analysis described by Noble & Tsien (1969*a*). The fully activated

current, $i_{x_1}$, is a non-linear function of potential that may be reproduced by the equation

$$\bar{i}_{x_1} = 1{\cdot}2(\exp[0{\cdot}04(E+95)]-1)/(\exp[0{\cdot}04(E+45)]) \qquad (22)$$

which is also based on using Adrian's (1969) model for inward-going rectification but with parameter values that prevent the current from declining towards zero at large depolarizations. The result, plotted in Fig. 1, is

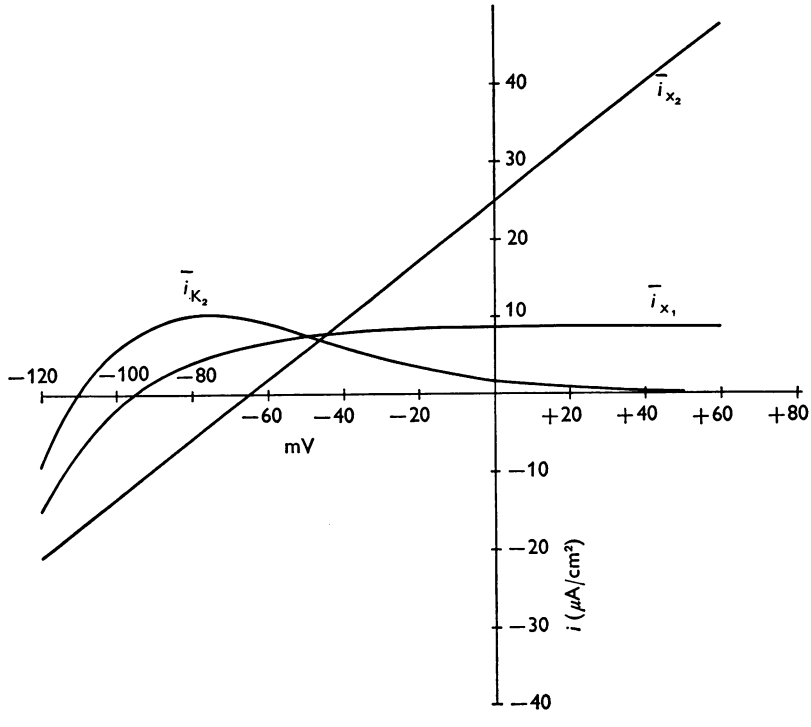


Fig. 1. Current–voltage characteristics of outward current components. Each curve gives the fully activated current–voltage relationship of a particular component when its 'channels' are fully open (gating variables equal to one). See eqns. (21), (22), (23).

similar to that obtained experimentally by Noble & Tsien (1969*a*, Fig. 9). The reversal potential measured by Noble & Tsien for $[K]_o$ = 4 mM was −84 mV. To give a relation appropriate to $[K]_o$ = 2·7 mM, we have shifted the reversal potential by −10 mV or so to −95 mV. This is based on observations by O. Hauswirth, D. Noble & R. W. Tsien (unpublished) that the reversal potential for $i_{x_1}$, is sensitive to $[K]_o$ although to a smaller degree than that for $i_{K_2}$.

The component $i_{x_2}$ was found to display a linear relation for the fully

activated current, with a reversal potential at approximately $-65$ mV (Noble & Tsien, 1969*a*). These features are reproduced by the equation

$$\overline{i_{x_2}} = 25 + 0{\cdot}385\, E. \tag{23}$$

Each of these components was found to obey simple first-order kinetics, so that eqn. (2) holds for the variables $x_1$ and $x_2$. These variables begin to turn on at about $-50$ mV ($i_{x_1}$) and $-40$ mV ($i_{x_2}$) and the channels are fully activated in the steady state at about $+20$ mV (Noble & Tsien, 1969*a*, Fig. 8). These features, and the voltage dependence of the time constants (Noble & Tsien, 1969*a*, Fig. 7) are reproduced by the rate equations given in Table 1.

*The transient chloride current, $i_{qr}$*

The involvement of chloride currents flowing during various phases of electrical activity in Purkinje fibres was demonstrated by Carmeliet (1961) and Hutter & Noble (1961). Their findings suggested that a small chloride current contributed to shortening the plateau duration (Carmeliet, 1961, Fig. 12; Hutter & Noble, Fig. 5) and to accelerating the rate of pacemaker depolarization (Hutter & Noble, 1961). The results were consistent with a time-independent chloride conductance with a reversal potential somewhere between the plateau and pace-maker voltage levels (see p. 20 below). In addition to this small but maintained chloride conductance, there was evidence from Carmeliet's (1961) experiments that a rather large chloride current might contribute transiently to the early repolarization from the peak of the spike to the beginning of the plateau.

A transient outward current did appear in the earliest voltage clamp experiments (Deck & Trautwein, 1964, Fig. 14; Hecht *et al.* 1964) with large depolarizations from the resting potential. Dudel, Peper, Rüdel & Trautwein (1967*a*) presented the first analysis of this current and, in particular, showed that it is greatly reduced by removal of chloride ions from the extracellular fluid. The time course of the outward current surge was consistent with an inactivation time constant of about 50 msec.

Further studies of the transient chloride current (Reuter, 1968; Peper & Trautwein, 1968) showed that recovery from inactivation required repolarization to near the resting potential and took place with a time constant of roughly 0·5–1 sec. These results further reinforced the earlier conclusion that the transient chloride current was largely responsible for the early repolarization, since the rapidity of the repolarization (and the appearance of a marked 'notch' configuration) are correspondingly sensitive to the interval between action potentials. At moderate to high action potential frequencies, the diastolic interval may be sufficiently short to severely limit the degree of repriming of $i_{qr}$ and, therefore, its participation

in the early repolarization (Reuter, 1968; Hauswirth, Noble & Tsien, 1972*a*).

Our formulation of the transient chloride current uses eqn. (5) where $q$ is the activation variable and $r$ is the inactivation variable. The current is labelled $i_{qr}$ rather than $i_{Cl}$ to clearly distinguish it from the small but maintained chloride conductance (see 'Background currents').

Relatively little experimental information is available on the activation process, and it is doubtful whether the onset of the transient has been reliably resolved. We have simply assumed that activation is directly proportional to $q$ to the first power. The rate constant expressions are based on the observations that the 'threshold' for the outward transient lies near $-20$ or $-15$ mV (Dudel *et al.* 1967*a*, Fig. 2; Reuter, 1968, Figs. 1, 10; Fozzard & Hiraoka, Fig. 2), and that the activation time constant is roughly 5–10 msec near 0 mV.

$$\alpha_q = 0{\cdot}008\, E/(1-\exp[-0{\cdot}1\, E]), \tag{24}$$

$$\beta_q = 0{\cdot}08 \exp[-0{\cdot}0888\, E]. \tag{25}$$

Considerably more experimental information has been presented for the inactivation process, $r$. Our equations are based on the experiments of Hauswirth *et al.* (1972*a*) who found a very slow removal of inactivation (time constant *ca.* 2 sec) in the diastolic range of potentials. The half-inactivation point ($r_\infty = \frac{1}{2}$) was located at $-80$ mV (cf. Hauswirth *et al.* 1972*a*).

$$\alpha_r = 0{\cdot}00018 \exp[-0{\cdot}04(E+80)], \tag{25}$$

$$\beta_r = 0{\cdot}02/(\exp[-0{\cdot}087(E+26)]+1). \tag{26}$$

The preceding expressions for $\alpha_r$ and $\beta_r$ were used for the bulk of the reconstruction results in this paper. After this work had been completed, a more extensive study of the inactivation kinetics became available (Fozzard & Hiraoka, 1973). Fozzard & Hiraoka's expressions for $\alpha_r$ and $\beta_r$ are as follows in units of msec$^{-1}$:

$$\alpha_r = 0{\cdot}000033 \exp[-E/17], \tag{27}$$

$$\beta_r = 0{\cdot}033/(1+\exp[-(E+30)/8]). \tag{28}$$

These equations locate the half-inactivation point at about $-55$ mV.

These expressions are similar in form to (25) and (26) but there are important quantitative differences which probably arise from a genuine experimental variability. The variability can be clearly seen in the electrical activity of individual preparations (Fig. 10), as well as in voltage clamp experiments. To emphasize that a range of behaviour is likely, we have carried out a limited set of calculations using the Fozzard–Hiroaka formulation for $r$ (Fig. 10*A*), and compared these results with those

produced with eqns. (35) and (36) in Fig. 9. Their formulation gives a notch which is less frequency-labile.

The fully activated current, $\bar{\imath}_{qr}$ has been described by

$$\bar{\imath}_{qr} = \bar{g}_{qr} \cdot (E - E_{Cl}), \tag{5}$$

where $\bar{g}_{qr} = 2{\cdot}5$ mmhos/cm$^2$ and $E_{Cl} = -70$ mV. The magnitude of $\bar{\imath}_{qr}$ was adjusted to give a realistic outward current surge under simulated voltage clamp conditions (see Fig. 13). The reversal potential level reflects the assumptions that the transient current is entirely carried by chloride ions and that chloride is passively distributed (see Hutter & Noble, 1961). The value of $-70$ mV is a rough estimate of the average potential level during the slow spontaneous activity which we have reconstructed. There is little direct evidence on the reversal potential, especially since many of the experimental determinations have been contaminated with $i_{si}$ (see Vitek & Trautwein, 1971). Reuter (personal communication) obtained a value of about $-70$ mV. Working in sodium-free solution, Fozzard & Hiraoka (1973) found a reversal potential of $-46$ mV. This value differs from the value we have assumed and from that measured by Reuter, but it is possible that their estimate may be influenced by residual $i_{si}$ (carried by calcium ions) or by level of holding potential in their experiments (usually $-70$ mV). Alternatively, it is possible that chloride ions are not passively distributed. The uncertainty about $E_{Cl}$ is not crucial since it is the *magnitude* of $\bar{\imath}_{qr}$ at positive potentials which is important to the reconstruction results.

*Background currents*

In their analysis of squid nerve membrane, Hodgkin & Huxley (1952) described a small residual current that remains when the time-dependent currents are accounted for. They called this component the 'leak' current. In squid axon, this appears as a linear current–voltage relationship (cf. Adelman & Taylor, 1961) with a reversal potential near the resting potential. The chief characteristics of 'leak' current is its lack of time-dependence, but it may be distinguished pharmacologically as well (see Hille, 1970).

Time-independent currents also remain in the analysis of current flow through muscle membranes. However, in both cardiac and skeletal muscle, the residual current–voltage relationship is quite non-linear, unlike that in nerve membrane. In referring to this current, we shall use the term 'background current' rather than 'leak current' since in cardiac electrophysiology the term 'leak' often describes the current flow in damaged regions of a preparation or in the sucrose regions of a sucrose gap system.

For the purpose of constructing normal activity, it is only necessary to describe the overall current–voltage characteristic of the background cur-

rent. This was the approach used by Noble & Tsien (1969*b*) in their simplified reconstruction of the plateau. However, some analysis of the ionic basis of the background current would obviously be important in understanding modifications or normal behaviour and in reproducing the effects of ionic concentration changes. We will specify the background current, therefore, in terms of constituent ionic components. This formulation is rather tentative, in the absence of reliable experimental means for dissecting the background current. It does not necessarily imply that genuinely distinct membrane channels exist for the various ionic components.

*Outward background current, $i_{K_1}$*

The outward component is mainly carried by potassium ions and corresponds to the outward membrane current that may be recorded below the threshold for $i_x$ in sodium-free solutions (see e.g. Hall *et al.* 1963, Fig. 2; Deck *et al.* 1964, Fig. 4). In sodium-free solutions the current carried by $i_{K_2}$ is absent or greatly reduced in amplitude near the resting potential (McAllister & Noble, 1966; see also discussion in Noble & Tsien, 1969*a*, p. 227). The rectifier properties of the background potassium current were investigated by McAllister & Noble (1966) who confirmed earlier observations that this component shows inward-going rectification, as assumed for the background current, $i_{K_1}$, in Noble's (1962*a*) model.

A very direct way of demonstrating that the outward background current is carried by potassium ions was described by Haas & Kern (1966) who measured the radioactive K efflux as a function of potential in a voltage clamped Purkinje fibre in sodium-free solution. They succeeded in showing that the current–voltage relation reconstructed from the flux measurements partly resembles that of the outward background current. It seems justifiable therefore to continue using the symbol $i_{K_1}$, for this current.

The equation we shall use for $i_{K_1}$ is

$$i_{K_1} = \overline{(i_{K_2}}/2{\cdot}8) + 0{\cdot}2(E+30)/(1-\exp[-0{\cdot}04(E+30)], \qquad (29)$$

which, like the equations for $\overline{i_{K_2}}$ and $\overline{i_{x_1}}$, is based on Adrian's (1969) rectification model with the addition of a 'constant field' component at large depolarizations. The parameters were chosen to give a current–voltage diagram similar to that obtained experimentally (McAllister & Noble, 1966; Dudel *et al.* 1967*b*).

It should be noted that any component of outward current resulting from electrogenic pumping may either be regarded as included in $i_{K_1}$ in this model, or, perhaps better, as reducing the value used for the inward background current.

*Inward background current*

The existence of a significant component of inward background current may be deduced from the fact that the resting potential ($-90$ to $-80$ mV) does not lie at the apparent potassium equilibrium potential (between $-115$ mV and $-100$ mV for $[K]_o$ values between 2·7 and 4 mM). Moreover, the magnitude of the inward component may be estimated by measuring the inward current required to hyperpolarize the membrane to $E_K$ (where the passive $K$ current is zero). Using this approach, Peper & Trautwein (1969, Fig. 4) found values of $1\text{–}2 \times 10^{-7}$ A at $E_K$. If a cylindrical surface area of 0·005–0·01 cm$^2$ is applicable to their experiment, the background current would be of the order of 20 $\mu$A/cm$^2$.

Although the inward background current plays an important functional role, its ionic basis is not completely clear. There is evidence from tracer studies that an appreciable sodium influx takes place in Purkinje fibres at rest. Bosteels & Carmeliet (1972) found a value of 15 pM/cm$^2$ of total membrane area, for the resting sodium efflux. This efflux is presumably attributable to the sodium pump, and should be balanced in the steady-state by an equivalent passive influx. Converting their value to units of current/cm$^2$ cylindrical fibre surface gives 17 $\mu$A/cm$^2$ for the background inward sodium current at the resting potential. This estimate would be proportionately lowered if some fraction of the sodium efflux were electrogenic (see Vassalle, 1970).

In the reconstruction we have used the following expression for the inward component of background current:

$$i_{Na,b} = \overline{g_{Na,b}}(E - E_{Na}) = 0{\cdot}105\ (E - 40). \qquad (30)$$

The value of $i_{Na,b}$ at the resting potential or at $E_K$ is in good accord with the experimental estimates of Bosteels & Carmeliet (1972) or Peper & Trautwein (1969). Equation (41) gives the linear current–voltage relation *a* in Fig. 2.

Although it seems reasonable to assign the inward background current to sodium ions, it should be noted that the cell membrane does not hyperpolarize to $E_K$ in sodium-free solutions (Draper & Weidmann, 1951; Dudel, Peper, Rüdel & Trautwein, 1966) although partial hyperpolarization is sometimes recorded (Hall *et al.* 1963, Fig. 1). It is possible of course, that substitutes for sodium, such as choline, may also pass through the inward background current pathway (Boulpaep, 1963; Bosteels, Vleugels & Carmeliet, 1970). This problem requires further experimental analysis since the inward background current is important, not only in helping to determine the resting potential in quiescent fibres, but also in pace-maker activity. The decay of $i_{K_2}$ can only lead to pace-maker activity if a steady inward current is present to generate the depolarization.

*Background current carried by chloride ions*

There is good experimental evidence that chloride ions contribute to the current flow during the pace-maker and plateau (see p. 31). We have described this presumably time-independent chloride component by the expression

$$i_{Cl,b} = \overline{g_{Cl,b}}(E - E_{Cl}), \tag{31}$$

where $E_{Cl} = -70$ mV. The parameter $\overline{g_{Cl,b}}$ was adjusted rather arbitrarily to give an action potential of representative duration (about 400 msec). We used a value of 0·01 mmhos/cm$^2$, which is probably unrealistic in the light of experimental results (Hutter & Noble, 1961; see p. 346). To carry out calculations aimed specifically at reconstructing chloride removal experiments, it would be appropriate to reapportion the outward background current, with a larger value of $i_{Cl,b}$.

*Total current–voltage diagrams*

Each of the individual components described above contributes to $i_1$, the overall membrane ionic current in the model. These contributions may be considered by plotting steady-state current–voltage relationships, as in Figs. 2 and 3. These diagrams show the cumulative effects of adding the steady-state current carried by individual components, one component at a time. Steady-state currents are calculated by setting the appropriate gating variable to its steady-state value. Thus,

$$(i_{K_2})_\infty = \bar{i}_{K_2} . s_\infty, \quad \text{where} \quad s_\infty = \alpha_s/(\alpha_s + \beta_s) \tag{32}$$

and so on for the other time-dependent currents.

Curve *h* in Fig. 3 shows the total steady-state current–voltage relationship for the model parameters used in the 'standard' action potential (see Fig. 4). This curve is N-shaped and may be compared with experimental current–voltage relationships obtained by use of the voltage clamp technique, which characteristically show a similar non-linearity. Note that the current–voltage relation intersects the abscissa at only one point, near $-38$ mV. This intersection is a stable point, but it is never attained during the reconstructed activity, due to the dynamic behaviour of the model.

Fig. 3 shows an additional current–voltage characteristic which is important to understanding the repolarization phase of the action potential. The dashed curve (curve *i*) is obtained by setting all kinetic variables to their steady-state values, with the exception of *s*, which is set equal to one. The result shows, therefore, the maximum possible contribution of the pacemaker potassium current, $i_{K_2}$, to the current–voltage relationship during repolarization (an experimental determination of the corresponding *I–V* relationship is given in Fig. 9 of Hauswirth *et al.* 1972*b*). Curve *i*

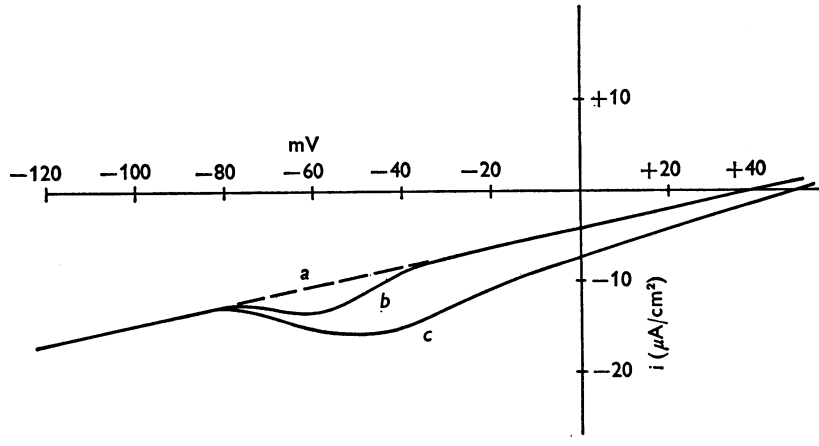


Fig. 2. Steady inward background current due to $i_{Na}$ and $i_{si}$. Current–voltage relationships (*a*, *b*, *c*) show the cumulative contributions of the components. *a*, time-independent background sodium current ($i_{Na,b}$); *b*–*a*, steady-state current $(i_{Na})_\infty$ carried by the excitatory sodium channels; *c*–*b*, steady-state current, $(i_{si})_\infty$ due to secondary inward current.

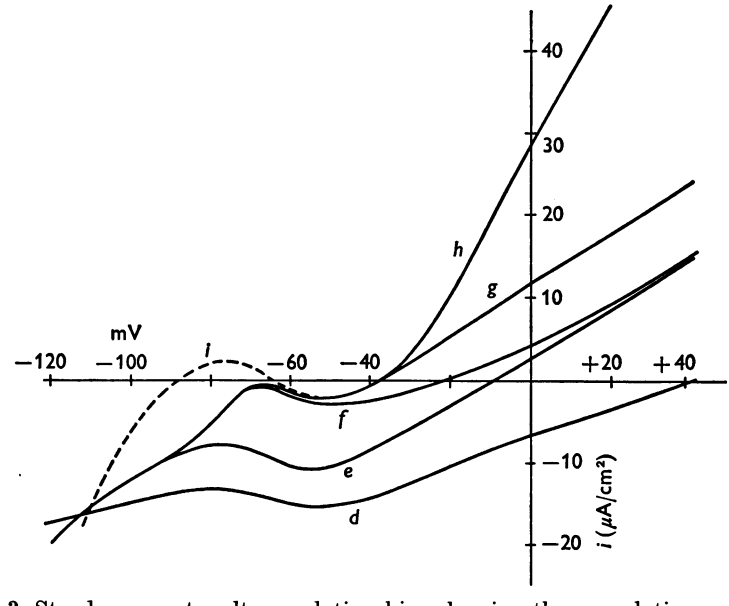


Fig. 3. Steady current–voltage relationships showing the cumulative contributions of outward current components to the overall steady-state current–voltage curve. *d*, $i_{Na,b} + (i_{Na})_\infty + (i_{si})_\infty + i_{Cl,b}$; *e*–*d*, $i_{K_1}$; *f*–*e*, $(i_{K_2})_\infty$; *g*–*f*, $(i_{x_1})_\infty$; *h*–*g*, $(i_{x_2})_\infty$; *i*, current–voltage relationship with $i_{K_2}$ fully activated ($s = 1$), while all other components are set at their steady-state values as in *h*.

intersects the abscissa at two potentials including a rather negative potential ($-88$ mV). The negative limb of the curve corresponds approximately to the behaviour of the ionic current during the repolarization phase of the action potential, which reaches a maximum diastolic potential approaching $-88$ mV (Fig. 4). Following the repolarization phase, the progressive deactivation of $i_{K_2}$ causes the current–voltage relationship to tend toward curve $h$, and eventually, the stable point in the pace-maker range of potentials disappears.

Another feature of the model shown in Fig. 3 is a region of steady-state inward current negative to $-38$ mV (in both curves $h$ and $i$). The existence of an inward current region may be somewhat surprising, since it would appear to prevent the termination of the plateau. This apparent difficulty is explained by the fact that the steady-state current–voltage curve is a poor estimate of the behaviour of $i_1$ during the termination of the plateau. During the calculated repolarization, the outward component $i_{x_1}$ is larger than its steady-state value, and the inward component $i_{s1}$ is smaller, so that the net ionic current is outward over the plateau range of potentials, as expected if repolarization is to occur.

## METHODS

Membrane action potentials and voltage-clamp currents were calculated using a general purpose computer program which has already been described (McAllister, 1970). Very briefly, the program uses the Runge–Kutta method to numerically integrate eqn. (1), together with the kinetic equations for the Hodgkin–Huxley-type variables ($m$, $h$, $s$, etc.). The computation incorporates automatic checks on accuracy, and varies the step length to achieve a compromise between accuracy and computing speed. No systematic attempt was made to optimize the parameters of the computation (cf. Moore & Ramon, 1974). Some of the preliminary calculations were made using an XDS Sigma 5 computer at Dalhousie University, but the results shown in the paper were carried out at Yale University using an IBM system 370 computer. A single action potential required about 2 min of computer time. The output was obtained in both numerical and graphical form: the plotted output was then traced to give figures in publishable form.

Many of the calculations involved variations in only one or two parameters. In an effort to keep all other aspects of the computation as similar as possible, we used two standard procedures for initiating membrane action potentials. In the first procedure, all activation variables ($m$, $s$, $x_1$, etc.) were set equal to zero, and all inactivation variables ($h$, $r$, and $f$) were set equal to one (this set of initial conditions is equivalent to that obtained by a strongly negative hyperpolarization which lasts long enough to set all variables to their steady-state values). The action potential was then initiated by displacing the membrane potential to $-50$ mV, that is well beyond the excitatory threshold. In the second procedure (see Fig. 6 and 13) all kinetic variables were set to their steady-state value at $-80$ mV. As in the first procedure, the action potentials were then initiated by a sudden depolarization to $-50$ mV.

Rectangular voltage clamp steps and the resulting membrane currents were calculated using McAllister's (1970) programme, and the results are shown in

Figs. 11–13). The gain of the model voltage clamp was 1000 mmhos/cm², and the maximal clamp current was set at 500 $\mu$A/cm². This would correspond to a maximal micro-electrode current of 1–5 $\mu$A for typically sized preparations used in voltage clamp experiment (right cylindrical areas ranging between 0·002 and 0·01 cm²). With this upper limit on the amount of clamp current, the theoretical voltage clamp is partly 'realistic' in the sense that the membrane capacitance cannot be charged up instantaneously, and the large surge of excitatory sodium current is not controlled. Step depolarization to the plateau range of potentials evokes an abortive action potential spike, giving way to recovered clamp control about 12–13 msec after the initiation of the step. The calculations were concerned with the subsequent changes in membrane ionic current which were smaller and slower and comparable to experimental recordings (see Fig. 13).

## RESULTS

### *PART I. RECONSTRUCTION OF THE ACTION POTENTIAL*

#### *The 'standard' action potential*

Fig. 4 shows the 'standard' action potential computed with model parameters as described in the previous equations. The action potential was initiated by a sudden displacement of membrane potential to −50 mV (see Methods). The calculated result is not intended to simulate any specific experimental recording; since the model parameters are based on a 'mosaic' of voltage clamp results, it is more appropriate to ask whether the model can readily reproduce the natural range of wave forms observed in Purkinje fibre action potentials. Later in this section we will describe more detailed comparisons between experimental and reconstructed activity. First, however, we shall draw attention to some of the important features of the 'standard' reconstructed action potential.

The action potential begins with a rapid upstroke that closely approaches the sodium equilibrium potential (+40 mV). Following the rapid depolarization, there is a fairly rapid repolarization to about −15 mV. The potential then moves again in a positive direction to −5 mV, thus generating the 'notch' that is characteristic of many experimental records (Draper & Weidmann, 1951; Carmeliet, 1961; Hauswirth *et al.* 1972*a*). We shall discuss the mechanism of this notch in more detail later, but it is worth remarking that this feature could not be reproduced in the model described by Noble (1962*a*).

The 'plateau' phase following the 'notch' follows a somewhat rounded (concave downwards) time course not dissimilar from many experimental records. This time course lies somewhere between the 'square' plateau (e.g. Draper & Weidmann, 1951, Fig. 4) and the 'triangular' repolarization wave (e.g. Dudel, Peper, Rüdel & Trautwein, 1967*c*, Fig. 5). We shall see later that it is relatively easy to generate the triangular wave form that often occurs in action potential without notches.

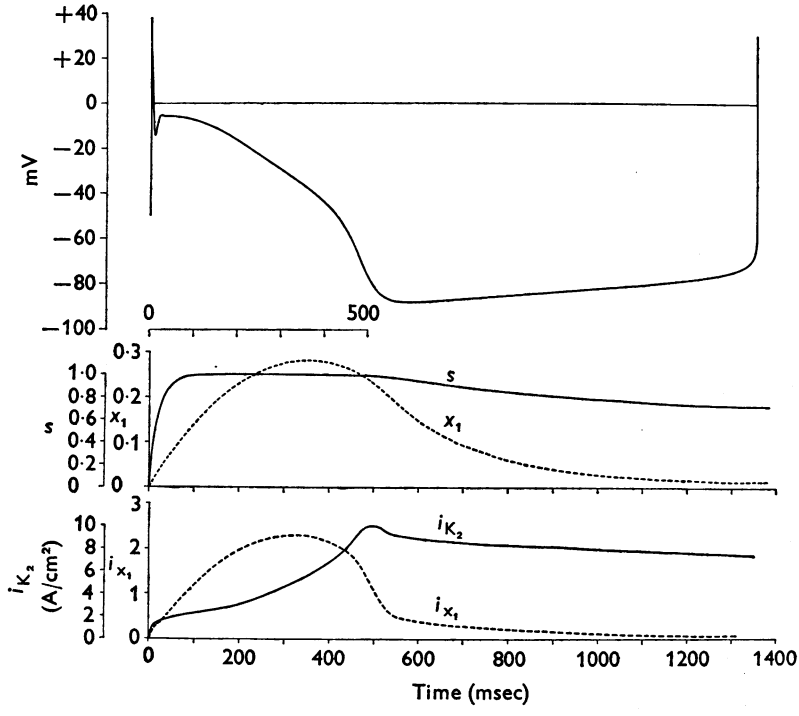


Fig. 4. Calculated action potential and pace-maker potential using 'standard' parameter values for 2·7 mM $[K]_o$. The action potential (top panel) was initiated by a sudden depolarization to −50 mV from a previous state where all activation variables were zeroed and all inactivation variables set equal to one (see Methods). The middle panel shows the time course of the Hodgkin–Huxley-type variables $x_1$ and $s$ which control the outward currents $i_{x_1}$ and $i_{K_2}$ respectively (lower panel). The vertical scales have been adjusted to emphasize the contrast in the components' time-dependent behaviour during the plateau and pace-maker potential.

Repolarization terminates at about 500 msec and gives way to the slow spontaneous depolarization (pace-maker potential).

The middle diagram in Fig. 4 shows the time courses of the activation of the gating variables $s$ and $x_1$ controlling the outward currents $i_{K_2}$ and $i_{x_1}$. The purpose of this diagram is to illustrate a further important respect in which the model differs from Noble's (1962*a*) model. In that model the activation and decay of a single potassium current ($i_{K_2}$) were responsible for controlling the time course of the plateau and pace-maker potential. In the present model, the activation of $i_{K_2}$ (controlled by the gating variable $s$) plays very little role in determining the plateau wave form for two reasons:

(*a*) The activation of $s$ is too rapid since it approaches 1·0 after only

50 msec. Thereafter $s$ is constant and there are no time-dependent variations in $i_{K_2}$.

(*b*) The value of $\overline{i_{K_2}}$ at potentials near zero is rather small (see Fig. 1) so that, even when the gates are fully activated, relatively little repolarizing current is contributed by this component.

The crucial time-dependent change in K current during the plateau is controlled by $x_1$ which reaches about 30 % activation towards the end of the plateau (cf. Noble & Tsien, 1969*b*).

During pace-maker activity, the roles are reversed. The decay of $x_1$ is not very important, partly because the decay is fairly rapid compared to the duration of the pace-maker depolarization but mainly because the pace-maker depolarization occurs at potentials close to the reversal potential ($-95$ mV) for $i_{x_1}$, so that $\overline{i_{x_1}}$ is fairly small (see Fig. 1, lower panel).

By contrast, the maximal current, $\overline{i_{K_2}}$, that can be carried by the $s$ channels is very large in the pace-maker range (see Fig. 1) and the decay of $i_{K_2}$ is similar to the time course of the pace-maker depolarization. This result confirms that obtained in the reconstruction described by Noble & Tsien (1968). However, it differs from, and extends, that result in an important way. Noble & Tsien *assumed* a time course for the pace-maker depolarization and computed the variation in $s$ and $i_{K_2}$ that would occur if the membrane potential was forced to follow the assumed time course. The result described here is one in which the time course of the pace-maker depolarization is in turn determined by the changes in $i_{K_2}$. Further consideration of the pace-maker mechanism will be deferred to Part III of this paper.

The behaviour of the other kinetic variables will be described in subsequent diagrams which focus on individual phases of electrical activity.

### *Reconstruction of the upstroke*

Fig. 5 (top) shows the first few milliseconds of the standard action potential plotted on a greatly expanded time scale in order to show the time course of the fast depolarization.

For comparison, Fig. 5 (bottom) shows the upstroke recorded experimentally in a dog Purkinje fibre by Draper & Weidmann (1951). The maximum rate of depolarization in each case is about 500 V/sec and the point at which the maximum rate is reached is about the same ($-10$ mV, indicated by arrow in left hand diagram). There are, however, two reasons for thinking that the agreement between the model and the experimental results is not as good as it may at first sight appear.

Firstly, Weidmann (1957) and many other investigators have also re-

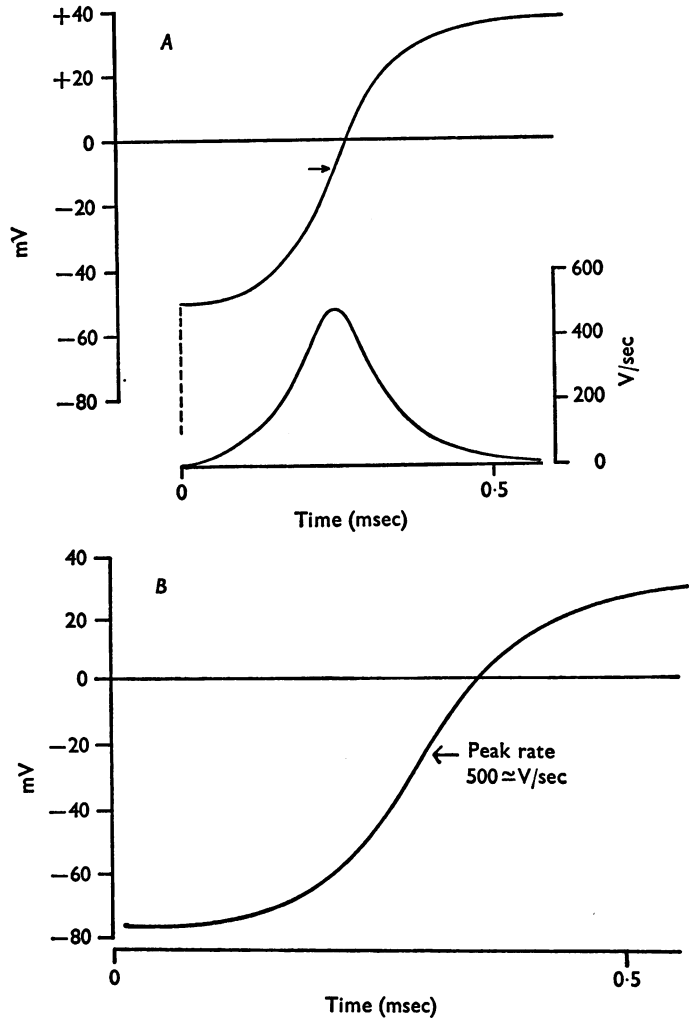


Fig. 5. *A*, the upstroke of the calculated membrane action potential (same calculation as Fig. 4) on an expanded time scale. The time derivative of voltage is shown below. The maximum rate-of-rise (478 V/sec) occurs when the potential reaches −8·9 mV (arrow). *B*, experimental action potential upstroke in dog Purkinje fibre (Draper & Weidmann, 1951) recorded under propagating conditions (see text).

corded upstrokes with depolarization rates of 800 V/sec, which is certainly beyond the range of values that may be reproduced by our equations.

Secondly, the methods by which the theoretical and experimental upstrokes are initiated in Fig. 5 are significantly different. The computed response is initiated by an instantaneous depolarization to −50 following

a 'pre-hyperpolarization' which sets $h_\infty = 1{\cdot}0$ (see Methods). The upstroke rate is therefore close to the maximal that the sodium current in the model can be made to generate. By contrast, the experimental record occurs after a slow spontaneous depolarization to $-75$ mV, at which $h_\infty$ is less than 1·0 (probably of the order of 0·75) so that the sodium current generated will be less than maximal. Moreover, it is likely that the experimental response is propagating along the fibre (unless, by chance, spontaneous excitation occurred synchronously) which also reduces the rate of rise (see Noble, 1962*b*).

When it is recalled that our equations already include a sodium conductance considerably larger than that measured in voltage clamp experi-

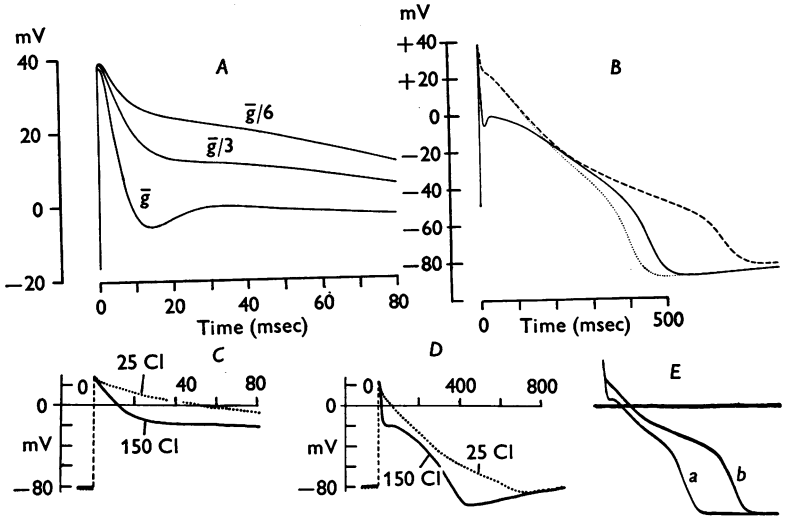


Fig. 6. The early repolarization phase and the effects of chloride removal *A* and *B* show reconstructed action potentials which were initiated by a sudden depolarization to $-50$ mV from a steady pre-potential of $-80$ mV. A, the early repolarization phase plotted on an expanded time scale. $\bar{g}$, chloride conductance parameters ($\overline{g_{\mathrm{qr}}}$ and $\overline{g_{\mathrm{Cl,b}}}$) set at 'standard' values; $\bar{g}/3$ and $\bar{g}/6$, chloride conductance parameters reduced to one third and one sixth, respectively. *B*, attempt at reconstructing the effect of chloride removal on the plateau. Solid trace shows the action potential with 'standard' parameter values. Dotted trace is obtained by repeating the calculation with chloride conductance parameters reduced to one sixth; dashed trace is similar but with an additional increase in background sodium current (see text). *C*, *D* and *E*, experimental recordings. *C* and *D*, the action potential and early repolarization phase in 150 mM chloride (continuous) and 25 mM chloride (dotted trace), from Dudel *et al.* (1967*a*). *E*: action potentials in normal chloride (*a*) and chloride-free (*b*) solution. from Carmeliet (1961).

ments (see *excitatory sodium current* above), it is evident that we are scarcely nearer to a satisfactory solution of this problem than in 1962, when Noble's model also failed to reproduce the very high rate of depolarization in Purkinje fibres.

*The early repolarization phase and 'notch'*

Fig. 6 compares our reconstruction of the early repolarization phase with experimental records. The computations were carried out with initial conditions rather similar to the experimental ones: the action potentials were initiated with a sudden depolarization to $-50$ mV, from a previous potential of $-80$ mV, where all kinetic parameters had been set to their steady-state values. The top left panel shows the calculated repolarization and ensuing 'notch' configuration. The maximum rate of repolarization ($-6{\cdot}47$ V/sec) is consistent with the reported results of Dudel *et al.* (1967*a*) although it is more rapid than the repolarization in their published record (Fig. 6, lower left).

The computed 'notch' time course is also similar to those recorded experimentally (see Fig. 7). In the reconstruction, the appearance of a marked notch depends upon the combination of two factors: first, the *de*activation of $i_{qr}$ as a consequence of repolarization to more negative potential; second, the progressive onset of $i_{si}$, which generates the secondary depolarization. Both of these processes are essential to giving a notch configuration (see 'Role of $i_{si}$ in notch and plateau').

*The effect of reducing the external chloride concentration*

The early repolarization and notch are very sensitive to changes in $[Cl]_o$. The effect of lowering the chloride concentration from 150 to 25 mM is shown in Fig. 6 (top right). This experimental result has been roughly simulated by calculating an action potential with the chloride conductance parameters ($\overline{g_{qr}}$ and $\overline{g_{Cl,b}}$) set to one sixth of their usual values, while leaving $E_{Ci}$ unchanged. The reduction in the transient chloride current has a marked effect on the computed repolarization phase, decreasing the maximum repolarization rate (from $-6{\cdot}47$ to $-1{\cdot}68$ V/sec). The extent of the early repolarization is also decreased in a manner that resembles Carmeliet's experimental recording (lower right) where the low-chloride trace bends sharply away from the control recording. This high 'plateau' in the action potential also appears in the reconstruction, where it arises from the secondary inward current. $i_{si}$ is operative in the normal action potential but its effect is further unmasked when $\overline{i_{qr}}$ is decreased.

Decreasing $\overline{i_{qr}}$ abolishes the notch configuration. The early repolarization falls short of deactivating $q$, so that there is a smooth progression from the

early repolarization phase to the plateau. The effect of reducing $\overline{i_{qr}}$ is similar to the effect of decreasing the outward transient current by inactivation at relatively rapid frequency rates (see p. 36).

Reducing the chloride conductance parameters to one sixth does not lengthen the action potential. The result contrasts with the lengthening observed experimentally (Fig. 6*E*). The absence of a prolongation in the calculated result is due to the extra activation of slow outward current ($i_{x_1}$) which occurs during the first 100 msec or so of the 'low-chloride' action potential, when the 'membrane' is more strongly depolarized. The extra outward current gives rise to a steeper repolarization over the plateau range of potentials. This also occurs in the experimental results (Fig. 6*D* and *E*), but only over the voltage range positive to $-20$ mV: the later phase of repolarization is markedly delayed, and hence the overall action potential duration is longer.

There are several possible explanations for the discrepancy. The most obvious one is that the chloride conductance $\overline{g_{Cl,b}}$ has been underestimated in the formulation of the 'normal' action potential model. This is probably the case since the value of $\overline{g_{Cl,b}}$ was chosen rather arbitrarily during the development of the model, and is much smaller than experimental estimates (see Hutter & Noble, 1961). With a more realistic value for $\overline{g_{Cl,b}}$, reduction of this parameter to one sixth normal would no doubt have a large effect in prolonging the duration of the calculated plateau.

Another possible explanation of the discrepancy is that chloride removal has an additional effect on ionic permeability which must also be incorporated in the reconstruction. In this context, it is worth noting that Dudel *et al.* (1967*a*) found an increase in tetrodotoxin-sensitive inward current when the external chloride was replaced by gluconate. They suggested that the maintained sodium current might also be augmented, judging from voltage clamp experiments with slowly changing ramps. A larger maintained inward sodium current would, of course, favour a longer action potential. Fig. 6*B* shows that a relatively small increase in the background sodium current would be sufficient to account for the prolonged plateau. The dashed trace shows a repeat of the 'low-chloride' calculation, but with $\overline{g_{Na,b}}$ raised from 0·105 to 0·120 mmhos/cm$^2$. The action potential duration is lengthened from 472 to 618 msec.

### *Role of $i_{si}$ in notch and plateau*

The development of a notch at the beginning of the plateau depends not only on the presence of a strong repolarizing chloride current (see above) but also on the presence of an inward current large enough to depolarize the membrane as the chloride current deactivates. This is illustrated in Fig. 7 (top left) which shows the effect of reducing the conductance $\overline{g_{si}}$ of the time-dependent second inward current. A sufficiently large reduction in $\overline{g_{si}}$ abolishes the notch, reduces the plateau height and shortens the action potential considerably (see Reuter, 1967). This pattern of behaviour suggests that, to a large degree, experimental variations in action potential shape may be due to variations in the magnitude of the second

inward current. The lower records in Fig. 7 show experimental records in two different dog Purkinje fibres by Draper & Weidmann (1951). The left-hand record shows a smooth repolarization time course with no notch; the right-hand record shows a marked notch and a higher plateau. Variation

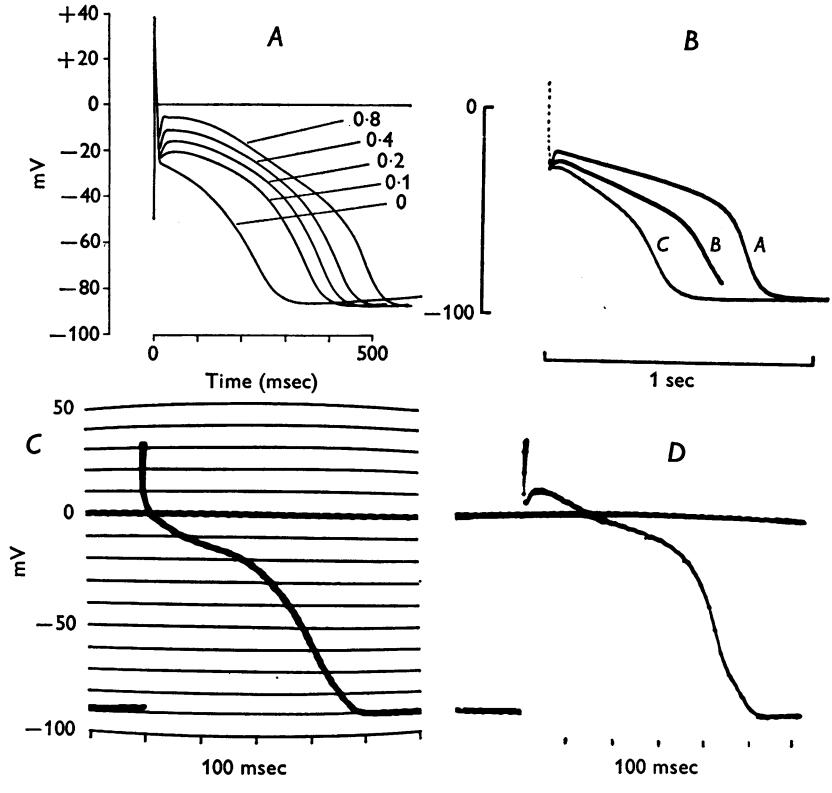


Fig. 7. The secondary inward current and the notch configuration. *A*, calculated action potentials showing the effect of varying the magnitude of the time-dependent secondary inward current. Trace labelled 0·8 is the same calculation shown in Fig. 4; other traces show the effect of reducing $\overline{g_{si}}$ from the 'standard' value. *B*, experimental action potentials showing progressive changes in configuration and plateau duration during the course of a single impalement (from Hauswirth *et al.* 1972*a*). Over a 20 min period the action potential became shorter and the notch configuration disappeared. *C* and *D*, experimental action potentials (Draper & Weidmann, 1951) displaying variability in the occurrence of the notch.

of this kind can also occur in the same fibre. Fig. 7 (top right) shows a series of three action potentials recorded at different times following a single impalement. Soon after the impalement, action potential (*A*) shows a marked notch, but over a 20 min period the action potential

progressively changes its configuration, and eventually shows no notch, a lower plateau and a shorter duration. These changes correspond well to those produced in the computed action potential by reducing $\overline{g_{si}}$.

Under certain circumstances, the magnitude of $i_{si}$ may be great enough to sustain an action potential without the aid of the fast sodium current. Fig. 8 (left) shows a calculated response with $\overline{g_{Na}} = 0$, initiated by depolarizing the 'membrane' with an applied 'current pulse'. The result is an action potential with an extremely low rate of rise (2·0 V/sec), no spike and no notch. For comparison, Fig. 8 right shows an experimental result obtained by Carmeliet & Vereecke (1969, Fig. 6*D*) in a sodium-poor solution (45 mM). Similar responses can also be obtained in sodium-free solution (Aronson & Cranefield, 1973), or when the fast sodium current is inhibited by tetrodotoxin or inactivated by depolarization in potassium-rich solution (Carmeliet & Vereecke, 1969; Cranefield, Wit & Hoffman, 1972).

The observation of Purkinje fibre action potentials in the absence of $i_{Na}$ has generally required some intervention to enhance the secondary inward current: elevation of $[Ca]_o$, exposure to adrenaline, or some similar manoeuvre. Since the model gives an 'action potential' without increasing $i_{si}$ above its 'normal' magnitude it is reasonable to ask whether this component has simply been overestimated. This is entirely possible, but in comparing experimental and theoretical results, one should recognize that the calculated responses are only 'membrane' action potentials, which do not necessarily fulfil the requirements for propagation in a cable (see Noble, 1972*b*). A reconstruction of propagated responses will be very helpful in determining whether or not the model parameters are experimentally realistic. Calculations performed with lower values of $g_{si}$ would give plateaus more dependent on $i_{Na}$ (cf. Draper & Weidmann, 1951).

### *Role of $i_{x_1}$ in controlling action potential duration*

The role of the potassium current, $i_{x_1}$ in the repolarization process has already been investigated by Noble & Tsien (1969*b*) in a preliminary, highly simplified model. Since the relevant features of the present reconstruction are based on the same experimental information as the earlier work, the role of $i_{x_1}$ remains unchanged. It will therefore be sufficient to briefly illustrate the important aspects.

The importance of time-dependent outward current is illustrated by computing the effect of abolishing $i_{x_1}$ and $i_{x_2}$ (Fig. 8). Although the notch and secondary depolarization are practically unaffected, repolarization fails to occur. This corresponds to the experimental finding (Noble & Tsien, 1969*a*) that the steady-state current–voltage relationship which remains

after subtracting off $i_{x_1}$ and $i_{x_2}$ shows a region of net inward current in the plateau range of potentials. According to this view, some activation of $i_{x_1}$ must take place before repolarization can occur.

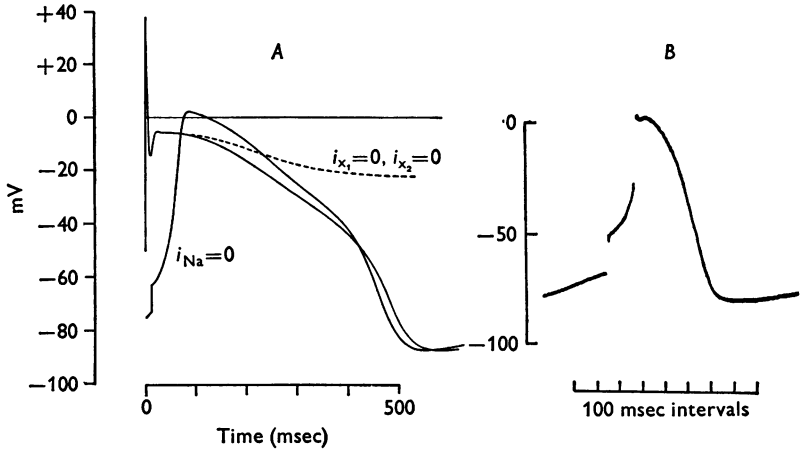


Fig. 8. The respective roles of $i_{si}$ and $i_{x_1}$ in generating the plateau and repolarization. *A*, the 'standard' action potential is compared with calculated responses in which specific components are omitted. In the absence of the excitatory sodium current ($i_{Na} = 0$), the secondary inward current can still support a membrane action potential, but without the usual initial spike. The dashed trace shows the result of abolishing the outward plateau currents ($i_{x_1} = i_{x_2} = 0$): normal repolarization is prevented and the potential is maintained within the plateau range by steady inward current (see text and Noble & Tsien, 1969*a*). *B*, experimental response of a cow Purkinje fibre in low-sodium solution (Carmeliet & Vereecke, 1969, Fig. 6*D*), in the presence of 11 $\mu$M adrenaline.

Another aspect of the functional role of $i_{x_1}$ is shown in Fig. 9. The standard action potential is followed (with an intervening interval of 200 msec) by a second evoked action potential. This 'extrasystolic' action potential is briefer than the first, 332 msec rather than 462 msec. The shortening of the second action potential depends on its 'proximity' to the repolarization phase of the first (see Gettes, Morehouse & Surawicz, 1972) and may largely be explained by the behaviour of $i_{x_1}$ (Hauswirth *et al.* 1972*a*). The lower panel displays the time course of the variable $x_1$ during the computed activity. At the beginning of the 'extrasystolic' action potential, $x_1$ is still residually activated ($x_1 = 0{\cdot}11$ in this particular example). During the course of the extrasystolic plateau, $x_1$ rises from this non-zero level and attains a peak value (0·35) which is significantly higher than the maximum value attained during the previous action potential (0·28). The time-to-peak $x_1$ in the extrasystolic action potential also occurs

at an earlier time (224 msec rather than 356) in rather good agreement with the over-all decrease in action potential duration.

*The effect of diastolic interval on action potential configuration*

It is clear in Fig. 9 that the reconstructed activity shows a dramatic dependence on the events previous to each action potential. Thus, the 'extrasystolic' and 'spontaneous' action potentials lack the marked notch configuration which appears in the 'standard' action potential. As discussed earlier (p. 32) this behaviour is often observed experimentally and may be attributed to the kinetics of repriming of the transient chloride

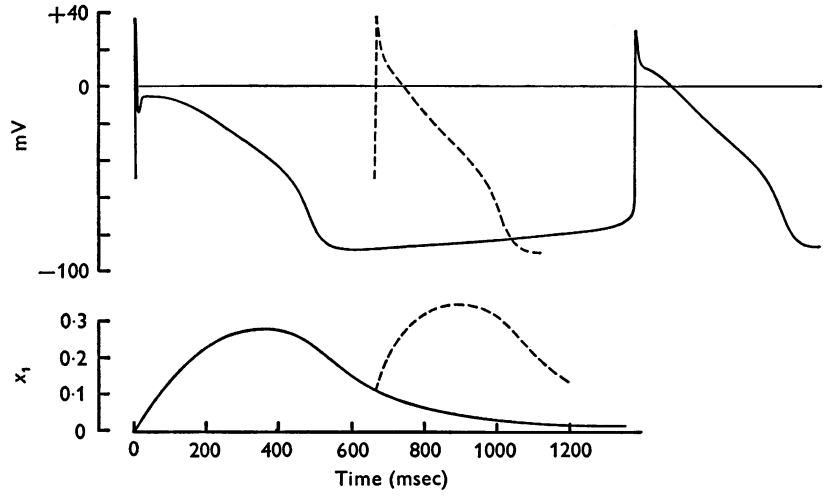


Fig. 9. The role of $i_{x_1}$ in controlling action potential duration. Top: calculated action potentials using 'standard' parameters, 'stimulated' by sudden depolarizations to −50 mV. The first action potential (same as Fig. 4) is followed by an extrasystolic response (dashed trace) which is briefer and lacking in the notch configuration. Bottom: the time-dependence of the underlying variation in $x_1$. In the extrasystolic response (dashed), $x_1$ begins at a non-zero value and attains a higher peak value during the ensuing plateau.

current, $i_{qr}$. Fig. 10 (middle) shows an example of a preparation where the notch only appeared after a period of quiescence lasting several seconds; stimulation at a relatively slow frequency (about 0·6 Hz) abolished the notch.

While this behaviour is fairly typical, it is also clear that there is a considerable variability. Fig. 10 (bottom) shows another preparation where a marked notch is displayed even at a relatively high frequency (about 1·7 Hz). These results were obtained under very similar conditions

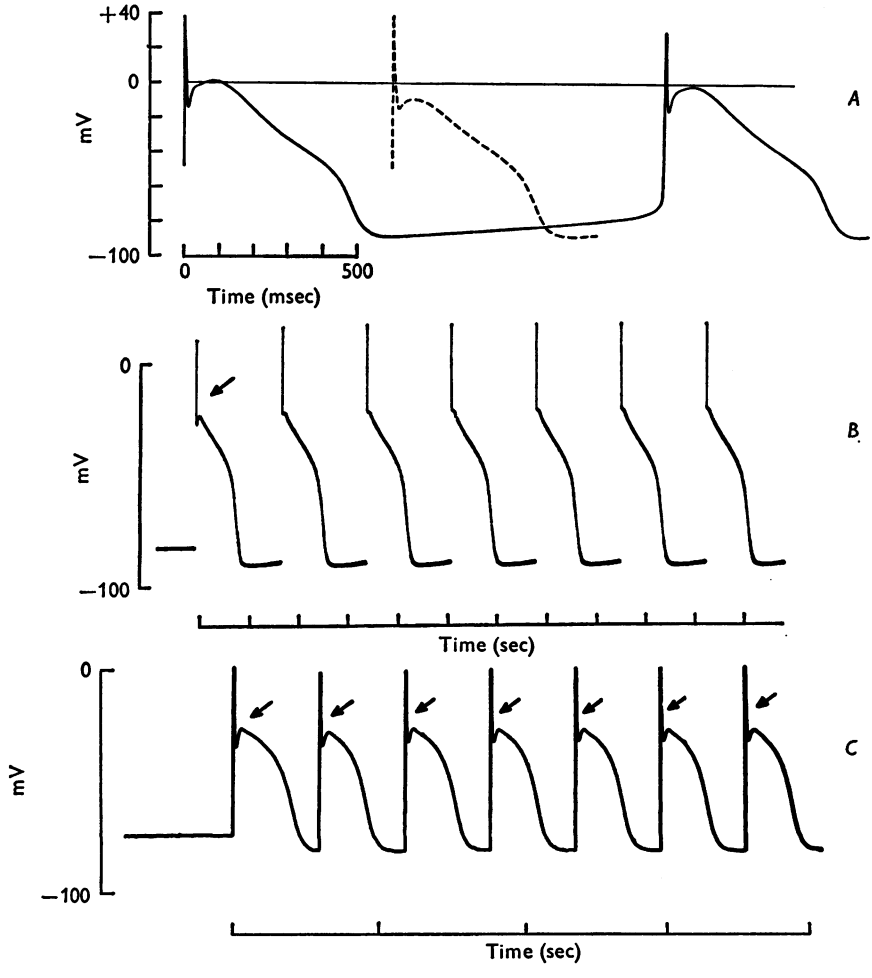


Fig. 10. The frequency-dependence of the notch and the repriming of the transient chloride component. *A*, calculations using Fozzard & Hiraoka's (1973) parameter values for $\alpha_r$ and $\beta_r$. Both the extrasystolic action potential (dashed) and the spontaneously generated action potential show a clear notch (contrast with Fig. 9). *B* and *C*, experimental recordings from sheep Purkinje fibre preparations, demonstrating the large variability in the frequency-dependence of the notch configuration. In both examples, a train of action potentials are externally stimulated after a prolonged ($> 20$ sec) quiescent period. *B*, a preparation where the notch (marked by arrow) is clear in the first action potential only (from Hauswirth *et al.* 1972*a*). *C*, another example, where the notch does not disappear even at a higher stimulation frequency (R. W. Tsien, unpublished).

using long sheep Purkinje fibre preparations, and there is no obvious explanation for the range of behaviour other than a genuine variability in the kinetic behaviour of one or more action potential currents.

This explanation is supported by voltage clamp studies of the chloride current $i_{qr}$ and its repriming characteristics (see p. 19). In particular, Fozzard & Hiraoka (1973) found a time course of repriming which was an order-of-magnitude faster than that described by model eqns. (25) and (26) which are based on the results of Hauswirth *et al.* (1972*a*). Fig. 10 (top panel) shows calculations of action potentials using the $\alpha_r$ and $\beta_r$ of Fozzard & Hiraoka (eqns. (27) and (28) of this paper). In this case the extrasystolic' and 'spontaneous' action potentials both show notch configurations, in agreement with the experimental recording in Fig. 10 (lower right). The reconstructed activity in Figs. 9 and 10 probably correspond to opposite poles of the experimentally observed range of behaviour. Other studies have suggested that the repriming of $i_{qr}$ takes place with a constant of about 0·5–1 sec (Peper & Trautwein, 1968; Reuter, 1968), a value which is midway between Fozzard & Hiraoka's data and the time constant found by Hauswirth *et al.* (1972*a*).

## *PART II. RECONSTRUCTION OF VOLTAGE CLAMP RESULTS*

Since our equations are based as closely as possible on the results of voltage clamp experiments, they necessarily reproduce the main features of voltage clamp current records. We shall not therefore describe such reproductions here. Instead we shall restrict ourselves to illustrating how the model simulates two particular phenomena. Firstly, we shall attempt to reproduce the all-or-nothing repolarization experiments described by Vassalle (1966) using short voltage clamp steps to displace the membrane potential during the plateau. These results have not been used in setting the equations and are a useful test of the model's range of validity.

Secondly, we shall illustrate how the model leads to an explanation of the fact that slowly developing outward current changes are sometimes difficult to observe at plateau potentials.

### *All-or-nothing repolarization experiments*

The phenomenon of all-or-nothing repolarization has been known for many years and was clearly demonstrated in Purkinje fibres by Weidmann (1951, 1956). His experiments, like those of Cranefield & Hoffman (1958) on ventricular muscle, were performed under non-uniform stimulating conditions. Although it is possible to reproduce the phenomena observed using cable models (Noble & Hall, 1963; Hall & Noble, 1963), the results are necessarily complex and are more difficult to relate to membrane ionic

currents than the results of uniform polarizations. Vassalle described such results in 1966, using short (20 msec) voltage clamp steps to polarize short Purkinje fibres to various potentials during the plateau phase. It is now clear that this duration is important in relation to the time required to deactivate $i_{si}$ which is necessary to initiate repolarization (see Reuter & Beeler, 1971).

Fig. 11 (middle) is one of Vassalle's records, showing the existence of a rather sharp threshold for all-or-nothing repolarization early in the plateau. A voltage-clamp pulse just short of threshold ($-60$ mV) is followed by a brisk depolarizing response that overshoots the original plateau level. On the other hand, a pulse just beyond threshold produces a repolarizing response that nearly attains the normal maximum diastolic potential, before giving way to a slow diastolic depolarization. The repolarizing response is not monotonic, but shows a temporary depolarization immediately after the voltage clamp circuit is shut off.

The detailed features of the experimental record are qualitatively well reproduced by the model. Fig. 11 (top) shows the response to four 'voltage clamp' steps to potentials near the calculated threshold. The arrow indicates the just supra-threshold response, whose calculation has been extended to show the subsequent pace-maker depolarization. The time elapsed between the shutting off of the 'clamp' and the next action potential is 930 msec, a value that nearly coincides with the diastolic interval (933 msec) after the 'standard' action potential (Fig. 4). This result is particularly noteworthy since the repolarization was initiated very early during the plateau. The fact that an early repolarization is followed by nearly full maximal diastolic potential and a normal pace-maker interval reveals that the process underlying pace-maker activity ($s$) is time-invariant during most of the plateau (see Fig. 4).

Experimental demonstration of this behaviour was available in Weidmann's early records (1951, Fig. 6). The development of a nearly normal maximum diastolic potential and pace-maker potential following premature repolarization could not be reproduced by Noble's (1962*a*) model, nor, indeed, in any model in which the onset and decay of the same potassium current mechanism are responsible for the repolarization and pace-maker respectively. Only in models in which the two phenomena are attributable to different current mechanisms can the current responsible for pace-maker depolarization be fully activated very early during the plateau. Weidmann's (1951) all-or-nothing repolarization experiments thus contained an important clue to suggest the existence of different kinetic processes controlling repolarization and pace-maker activity in Purkinje fibres.

The distinction between subthreshold and suprathreshold behaviour is

less sharp at a later stage in the plateau. Fig. 11 (top) shows calculated responses to 'voltage clamp' steps applied 180 msec after the beginning of the action potential. The clamp pulse to −43 mV (arrow) is clearly

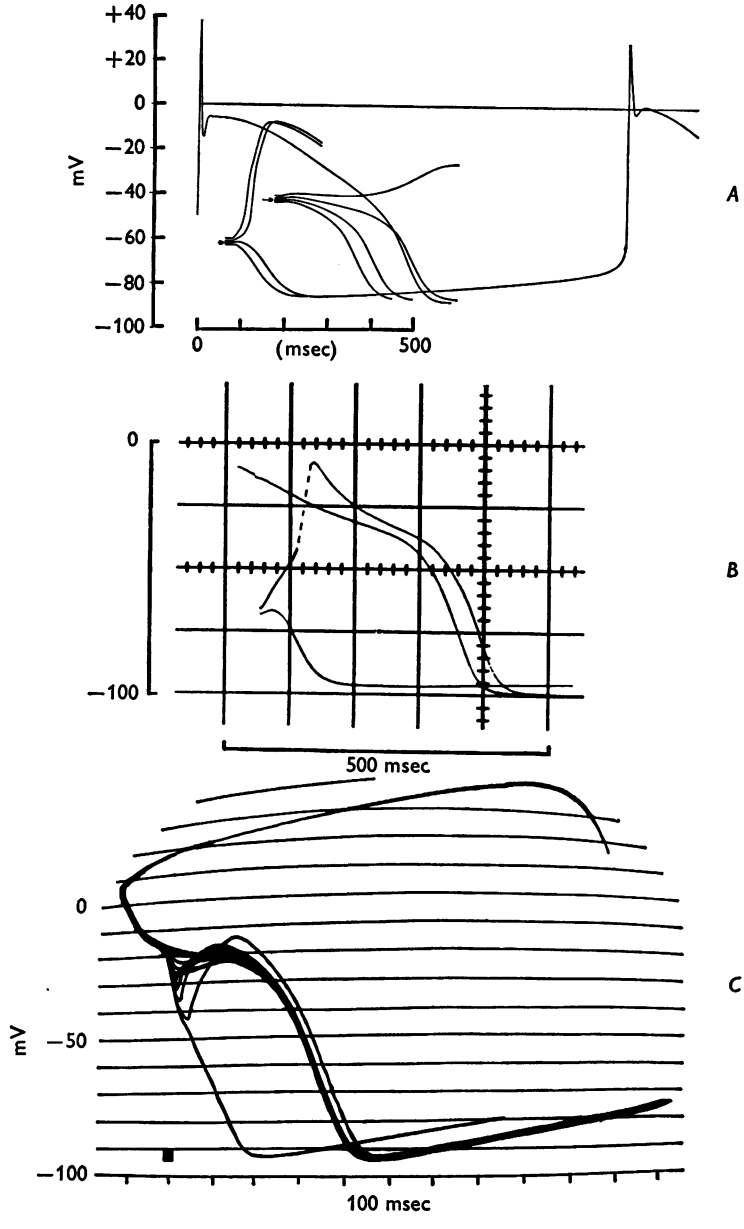


Fig. 11. For legend see facing page.

beyond threshold, and gives a repolarizing response. Clamping to −41 mV clearly falls short of threshold since the response consists of a slow depolarization that extends well beyond the normal plateau duration. The clamp pulse to −42 mV succeeds in producing a repolarization, but this response intersects the normal action potential. It seems reasonable to regard responses which cross the action potential as subthreshold, and therefore, in this case the threshold value to the nearest millivolt is −43 mV. Even later in the plateau (240 msec) no threshold can be defined. Any hyperpolarization will tend to hasten the repolarization process. This agrees qualitatively with Vassalle's published record (Fig. 12, right) where no threshold can be defined for the later portion of the action potential.

Fig. 12 compares the time course of all-or-nothing threshold as determined

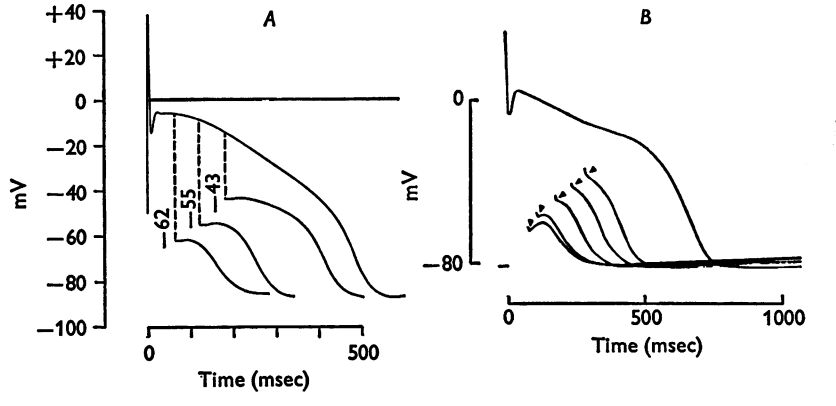


Fig. 12. The time dependence of the threshold for all-or-nothing repolarization, (*A*) for the reconstructed action potential and (*B*), as determined experimentally (Vassalle, 1966).

---

Fig. 11. The phenomenon of all-or-nothing repolarization. *A*, determination of the threshold for repolarization, using the 'standard' action potential. At 60 msec, the 'membrane' is effectively voltage clamped for 20 msec to potential levels −60, −61, −62 and −63 mV. The step to −62 is followed by a repolarizing response, and is therefore marked (arrow) as suprathreshold (note that the premature repolarization is nevertheless followed by a normal pace-maker depolarization: see text). The clamp steps to −60 and −61 mV fall short of threshold and are followed by depolarizing responses which overshoot the original plateau (cf. *B*). At 180 msec the threshold is less clearly definable. The clamp step to −43 mV (arrow) is designated by convention as 'suprathreshold' since it produces an earlier repolarization than in the original action potential. *B*, experimental determination of threshold using the voltage clamp in a shortened preparation (M. Vassalle, unpublished). *C*, all-or-nothing repolarization in a long preparation (Weidmann, 1951), showing the pace-maker behaviour following a premature repolarization.

experimentally and theoretically. The left hand panel shows calculated just-suprathreshold responses to 20 msec 'clamp' steps at 60, 120 and 180 msec. The computed threshold shifts toward the plateau potential with time, in a manner that strongly resembles Vassalle's experimental result (right panel). In both cases the threshold ceases to exist at a point midway during the plateau. In the reconstructed result, the progressive change in threshold voltage corresponds to the onset of $i_{x_1}$, which gradually overcomes the residual inward current in the plateau range of potentials (see Noble & Tsien, 1969*b*, Fig. 2).

*Current changes during voltage clamp steps to the plateau potential range*

A major problem in the analysis of the earliest voltage clamp results was the lack of correlation between current changes *during* depolarizing clamp pulses and current changes *following* them. Despite strong evidence that a time-dependent decay of potassium current occurred after a depolarizing clamp pulse, the current records during the pulse often failed to show a slow increase in outward current. Indeed, they often showed a decrease (see, for example, Deck & Trautwein, 1964, Fig. 6; Reuter, 1967, Fig. 5).

One reason for this problem is now clear. During strong depolarizations there is a large outward transient current (see *The chloride current*, $i_{qr}$, above) which may be large enough to mask the relatively small and slow changes in potassium current. Fig. 13 illustrates this by simulating voltage clamp depolarizations to potentials in the plateau range. The voltage levels are superimposed together with the wave form of an action potential which was initiated from the same starting level ($-80$ mV).

The clamp depolarizations ($-10$, 0 and $+10$ mV) span the voltage range over which the component $i_{qr}$ becomes activated. The smallest depolarization ($-10$ mV) is just sufficient to activate some $i_{qr}$; only a small outward current surge appears, and this gives way to an inward current peak (due to $i_{si}$ which slowly declines ($i_{si}$ inactivation and $i_{x_1}$ activation). The strongest depolarization ($+10$ mV) produces a large outward current surge which peaks at 20·7 msec and then decays (the time-to-peak is in good agreement with experimental results – see Dudel *et al.* 1967*a*, Fig. 3). Although the calculated current record includes an appreciable secondary inward current, the net current is clearly dominated by the time-dependent behaviour of $i_{qr}$. Closer inspection of the calculated current shows a slight increase in outward current during the last 300 msec of the pulse. Although this could easily be overlooked, the onset of outward current is crucial in terminating the plateau of the reconstructed action potential (see Fig. 8).

This comparison between action potential and voltage clamp behaviour, using the same membrane model, illustrates how the voltage clamp results can be misleading. Although $i_{qr}$ appears quite dominantly in the current

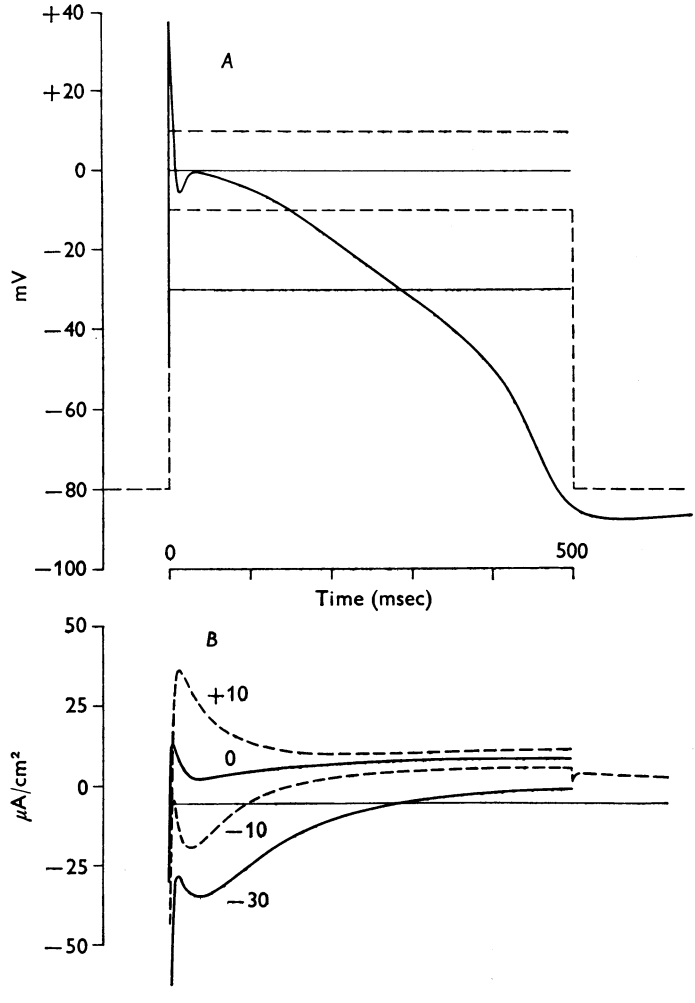


Fig. 13. Reconstruction of a voltage clamp experiment studying plateau currents. *A*, the simulated voltage clamp pulses (superimposed). Each pulse steps the membrane voltage from the same holding potential (−80 mV) to a different level within the plateau range. An action potential (Fig. 6) with the same model parameters and initial condition is also superimposed as a reference (in each reconstructed clamp, the potential undergoes an abortive spike during the first few milliseconds when the sodium current is too large to be 'controlled' by the applied current (see Methods). The spikes would have appeared as a thick vertical line and are omitted for the sake of clarity). *B*, the resulting current records. These traces are dominated by the outward chloride transient (pulse to +10) or the secondary inward current (pulse to −30). The phasic components of outward and inward current can overlap (pulse to 0) and give rise to an apparent 'reversal potential' (see text). The thin horizontal line shows the steady holding current at −80 mV.

records, its role in the action potential is much more restricted because the chloride transient deactivates itself via its action to repolarize the membrane. Following the action potential crest, $i_{qr}$ activates quickly and generates a brisk repolarization to potential levels where it then *de*activates (Dudel *et al.* 1967*a*). Since deactivation takes place much more rapidly than inactivation ($\tau_q \ll \tau_r$), the overall duration of the chloride transient is much briefer in an action potential than during a voltage clamp pulse. The flow of $i_{qr}$ is primarily restricted to the first 10–20 msec when the early repolarization and notch occur.

The intermediate voltage clamp step (to 0 mV) produces neither a large outward nor a large inward current surge. At this potential, $i_{qr}$ and $i_{si}$ roughly cancel each other out. It is clear that the pattern of current changes in Fig. 13 might easily be mistaken as evidence for the existence of a single current component with a reversal potential near the plateau level (see Peper & Trautwein, 1968; Vitek & Trautwein, 1971; Trautwein, 1973).

## *PART III. PACE-MAKER ACTIVITY*

The mechanism of pace-maker activity produced by the model (see Fig. 4) is similar (though not identical – see below) to that described by Noble & Tsien (1968). The primary time-dependent process is the decay of $i_{K_2}$, which allows the inward background current to depolarize the membrane towards the sodium threshold. The membrane conductance therefore decreases during the pace-maker depolarization, as observed experimentally by Weidmann (1951). The time-dependent fall in $i_{K_2}$ is not however the sole explanation for the resistance changes. Two other factors are also involved: (*a*) the voltage-dependent decrease in $\overline{i_{K_2}}$ and (*b*) the partial activation of $i_{Na}$ as the threshold for spike initiation is approached. Both of these phenomena introduce negative conductance properties towards the end of the pace-maker depolarization and, in experiments using constant current pulses, they have the effect of increasing the measured membrane resistance. The fall in $\overline{i_{K_2}}$ on depolarization has already been discussed earlier in the paper. The partial activation of $i_{Na}$ is also an important aspect of the model which will be discussed later in this section ('Reconstruction of the effect of calcium ions').

The results which follow will focus specifically on pace-maker activity and the reconstruction of the chronotropic effects of single current pulses, adrenaline, and calcium ions.

### *The chronotropic effects of current pulses*

While using small current pulses to monitor changes in membrane conductance during pace-maker activity, Weidmann (1951) made an interesting and unexpected observation. He noticed that single short

subthreshold depolarizing pulses *slow* the approach to threshold, while similar hyperpolarizing current pulses *speed* the approach to threshold. At first sight these results may be puzzling since the charge actually applied would tend to favour the opposite result to those that were actually observed. Moreover, although this was not noticed at the time, Noble's (1962*a*) model is unable to reproduce Weidmann's result.

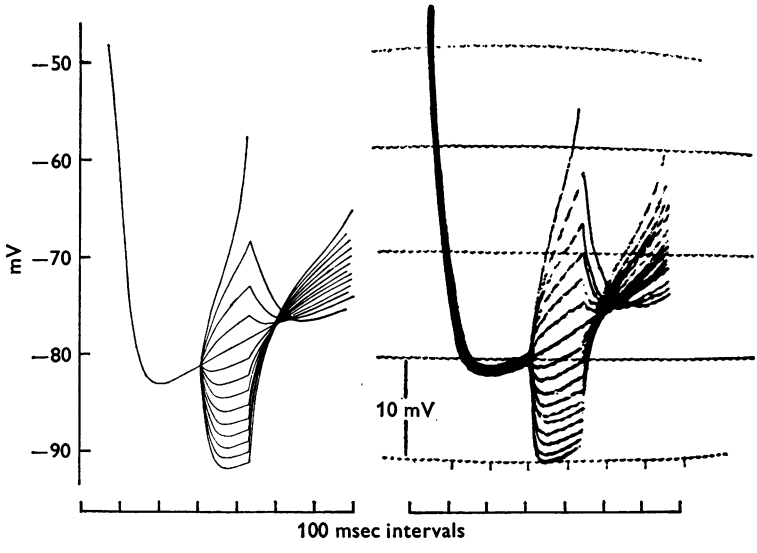


Fig. 14. Chronotropic effects of short current pulses. *Left*, computed effects of depolarizing and hyperpolarizing current pulses applied during the pace-maker potential. Note that subthreshold depolarizing currents slow the subsequent approach to threshold, whereas hyperpolarizing pulses speed the subsequent depolarization (computed from our model by O. Hauswirth, 1971). *Right*, experimental records obtained by Weidmann (1951).

McAllister & Noble (1967) suggested that the phenomena might be explained by the fact that the pace-maker potassium current is very sensitive to membrane potential over the range of the pace-maker depolarization (i.e. $s_\infty(E)$ is very steep). Relatively small current pulses can therefore strongly activate or deactivate $i_{K_2}$, and so have an appreciable chronotropic effect. This suggestion is amply confirmed by the results shown in Fig. 14. The left-hand records show the computed effects of small pulses applied during pacemaker activity. These results were computed by Dr O. Hauswirth using an earlier version of our model (for details of the equations used, see Hauswirth, 1971). The equations for $i_{K_2}$ are the same as given in the present paper, although the sodium current equations differed slightly. The right-hand records are taken from Weidmann's (1951) experimental results.

*Reconstruction of the pace-maker action of adrenaline*

Hauswirth, Noble & Tsien (1968) have shown that adrenaline shifts the activation curve for $i_{K_2}$ in a depolarizing direction, by as much as 25 mV (see also Tsien, 1974). This voltage shift may be contrasted with the lack of effect on $i_{Na}$ (Trautwein & Schmidt, 1960). We have investigated the effect of similar voltage shifts in $i_{K_2}$ on the computed pace-maker activity

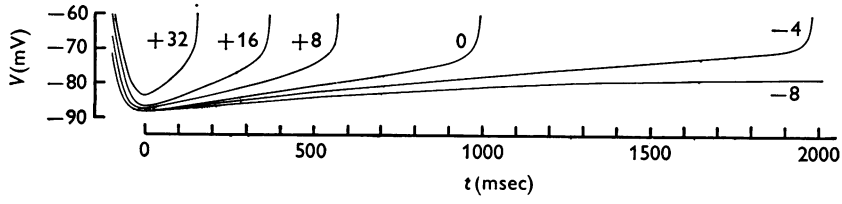


Fig. 15. Reconstruction of the acceleratory effect of adrenaline on pace-maker activity. The effect of adrenaline is simulated by displacing the rate coefficients $\alpha_s$ and $\beta_s$ along the voltage axis toward less negative potentials. The magnitude of the displacement (in millivolts) is indicated for each trace. The pace-maker depolarization under 'standard' conditions (no displacement) is labelled 0.

(Fig. 15). In each computation only the pace-maker depolarization is shown. We have not attempted to reproduce changes in the action potential plateau since it is now clear that these are dependent on other actions of adrenaline, i.e. modifications of $i_{x_1}$ and $i_{si}$ (Tsien, Giles & Greengard, 1972). Such changes are not included in the present reconstruction but we can be confident that they will have no significant effect on the results. The degree of activation of $i_{K_2}$ at the beginning of the pace-maker depolarization is virtually independent of the events occurring during the action potential. As shown earlier (Fig. 4) $s$ approaches full activation within the first 50 msec.

It can be seen from Fig. 15 that even very small shifts in the voltage dependence of $s$ produce marked changes in the duration of the pace-maker depolarization. This corresponds well to the experimental observation that the pace-maker is sensitive to concentrations of adrenaline well below that used by Hauswirth, Noble & Tsien (1968) to produce a 25 mV shift (i.e. 1·5 $\mu$M).

There is one major respect in which the computations shown in Fig. 15 do not reproduce the action of adrenaline at potentials in the normal pace-maker range. In experimental recordings (Otsuka, 1958) the maximum negative potential reached at the end of repolarization normally becomes more negative, whereas in the computations, the maximum negative potential is less negative when the $s$ activation curve is shifted in a de-

polarizing direction. This discrepancy is interesting because it suggests that adrenaline has some additional effect that has not been incorporated in the reconstruction. The nature of such an effect has already been suggested by Vassalle in his studies of electrogenic sodium transport in Purkinje fibres. The electrogenic pump provides increased outward (i.e. hyperpolarizing) background current in response to an elevation in impulse frequency (Vassalle, 1970) and also as a result of a direct stimulatory effect of catecholamines on the pump (Vassalle & Barnabei, 1971). The eventual hyperpolarization of the maximum diastolic potential (Otsuka, 1958) is thus largely a secondary effect of the increased automaticity (and presumably, an elevated internal sodium concentration). This hypothesis is further supported by the observation that adrenaline produces a transient reduction of the maximum diastolic potential (in accord with the computer results) before the eventual hyperpolarization. Further experimental work will be needed before changes in the electrogenic pump current can be incorporated in the reconstruction.

*Reconstruction of the chronotropic actions of calcium ions*

Calcium ions resemble adrenaline in their action on the pace-maker potassium current. The activation curve of $i_{K_2}$ is displaced in the direction of less negative potentials by increasing the external calcium concentration (D. Noble & R. W. Tsien, unpublished; Brown & Noble, in preparation). If this action were the only one, elevations in $[Ca]_o$ would necessarily mimic the positive chronotropic effect of adrenaline. Since a fourfold change in $[Ca]_o$ shifts the activation curve for $i_{K_2}$ by about 8 mV, a significant acceleration would be expected, and as shown in Fig. 15, the diastolic interval should be markedly decreased.

This expectation is contrary, however, to Weidmann's (1955*b*) experiments where raising $[Ca]_o$ actually *prolonged* the diastolic interval. Fig. 16 shows a particularly illustrative example of this effect, recorded by P. Müller (see Weidmann, 1964). Elevating $[Ca]_o$ does steepen the early pacemaker depolarization, as expected (see also Temte & Davis, 1967) but there is also a marked displacement in the potential from which the upstroke 'takes off', and an overall *increase* in the diastolic interval. The displacement of the 'threshold' suggested that the excitatory sodium current is also sensitive to $[Ca]_o$. Weidmann (1955*b*) found that the activation process ($m$, as judged by the 'threshold') and the inactivation process ($h$) appear to be similarly affected. His average results showed a 6 mV shift for the 'threshold' and a 5·6 mV shift for the location of the $h_\infty(E)$ curve.

The influence of calcium ions on the sodium current kinetics is appropriate to counteract the effect on $i_{K_2}$ activation, since larger depolarizations would be required to reach threshold. The over-all chronotropic effect

depends critically, however, on the quantitative balance between the individual effects. It seems, therefore, that the reconstruction of $[Ca]_o$ action is a worthwhile application of the computer model.

*Contributions of changes in $i_{K_2}$ and $i_{Na}$ to the pacemaker potential.* Before attempting a reconstruction of the action of $[Ca]_o$ it is important to clarify the contribution of various current changes to the pacemaker. Fig. 16

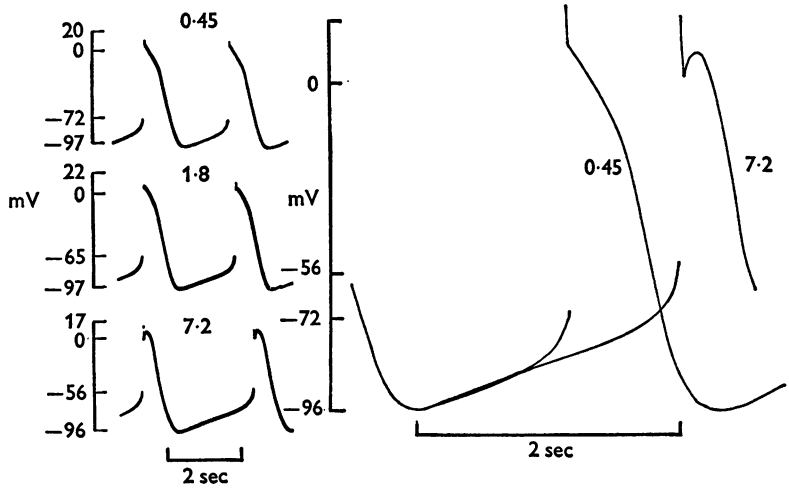


Fig. 16. The effect of calcium ions on pace-maker activity (recorded by Professor P. Müller and reported in Weidmann, 1964). *Left*, the panels show recordings from a single preparation in different calcium concentrations: 0·45 mM (top), 1·8 mM (middle) and 7·2 mM (bottom). Increasing $[Ca]_o$ slows the spontaneous activity through a change in the 'threshold' level (see left-hand scale). Note, however, that the *initial* slope of the pace-maker depolarization is steepened by elevating $[Ca]_o$ (see also Temte & Davis, 1967). *Right*, superimposed tracings of records in 0·45 and 7·2 mM-$[Ca]_o$.

provides an important clue to such an analysis. It shows that the slow diastolic depolarization gives way to a progressively steeper depolarization, lasting about 100 msec before the upstroke and spanning the last 10–15 mV negative to the point where the oscilloscope trace disappears. In this experiment, the late upswing is displaced by variations in calcium concentration in the same manner as the 'threshold' itself. It appears then that *at least* 100 msec of the diastolic interval is sensitive to the activation of sodium current, and may therefore contribute to the net effect of $[Ca]_o$.

Fig. 17 pursues this point by showing computed pace-maker depolarizations together with the concurrent changes in $s$, $i_{K_2}$, and $i_{Na}$. The sodium current kinetics have been adjusted for the normal calcium concentration

in Tyrode $[Ca]_o$ = 1·8 mM, and hence $h_\infty$ = 0·5 for $E$ = −73·5 mV (see p. 10).

Deactivation of $i_{K_2}$ dominates the overall current change during the early portion of the diastolic depolarization. About midway in the diastolic interval, the onset of $i_{Na}$ becomes appreciable, and for some 300 msec before the upstroke, the magnitude of the increase in $i_{Na}$ is comparable to the decrease in $i_{K_2}$. In fact, the change in $i_{Na}$ becomes significant well

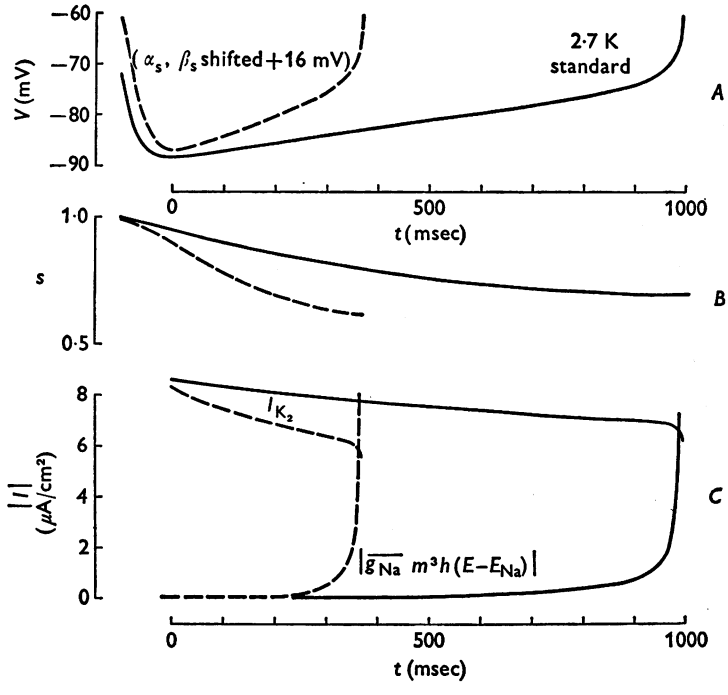


Fig. 17. Computed pacemaker potentials and the underlying current changes. *A*, calculations of 'standard' pace-maker activity (continuous) and with the rate coefficients $\alpha_s$ and $\beta_s$ shifted by +16 mV toward less negative potentials (dashed trace), as in Fig. 15. *B*, the corresponding time-dependent changes in $s$. The acceleratory effect is generated by a more rapid and more complete deactivation of the variable $s$ in the dashed trace. *C*, the time course of $i_{K_2}$ and $i_{Na}$. As the potential approaches −70 mV, the excitatory sodium current is progressively activated. This, together with a fall in $i_{K_2}$ (due to inward-going rectification) leads to the increase in net inward current that generates the last phase of the pace-maker depolarization.

*before* the potential shows signs of swinging upward. In the reconstructed pace-maker potential, therefore, a surprisingly large fraction of the total diastolic interval is dependent on the sodium current kinetics. In this

respect, the present account differs from an earlier paper (Noble & Tsien, 1968) where the late upswing was attributed to the negative slope in the relation between $\overline{i_{K_2}}$ and membrane potential. The latter must certainly contribute but does not play the unique role suggested by Noble & Tsien (1968).

*Reconstruction of* $[Ca]_o$ *effects.* Fig. 17 suggests that displacements in the location of the sodium kinetic parameters may have a rather large influence on the diastolic interval. We have investigated, therefore, the chronotropic effects of $[Ca]_o$ by simulating the displacements in $i_{Na}$ and

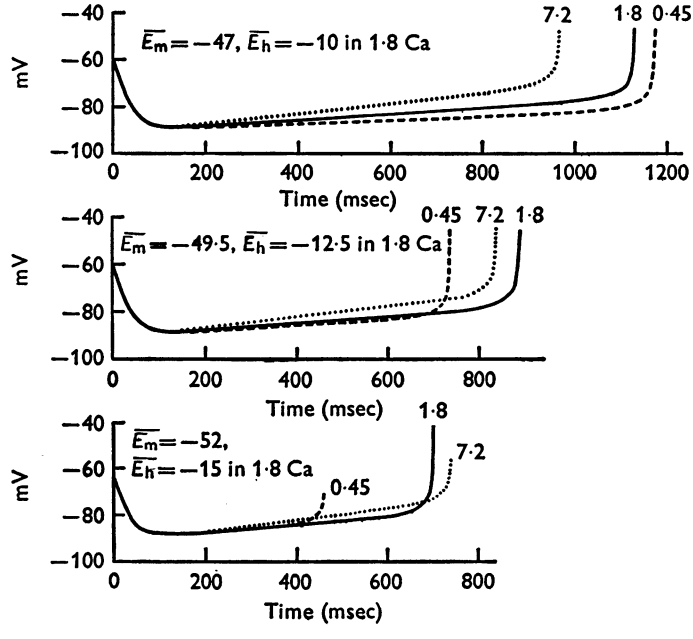


Fig. 18. Reconstruction of the effect of calcium ions on pace-maker activity. Each panel shows the result of shifting the kinetic parameters of $i_{Na}$ and $i_{K_2}$ by appropriate amounts to simulate the effect of fourfold variations in $[Ca]_o$. The top panel shows the chronotropic effect when the sodium kinetics are located at their 'standard' position while in '1·8 mM calcium' solution. The middle and lower panels are obtained by relocating the sodium kinetics in '1·8 mM calcium' at more negative levels, and thus accentuating the relative importance of $i_{Na}$ in determining the total diastolic interval. For further explanation see text.

$i_{K_2}$ in computer reconstructions of the pace-maker. In accord with the experimental results, the curves for $\alpha_m$, $\beta_m$, $\alpha_h$ and $\beta_h$ were each shifted along the voltage axis by +6 mV in '7·2 mM calcium', while $\alpha_s$ and $\beta_s$ were shifted by +8 mV. In '0·45 mM calcium', the rate constants were shifted by corresponding amounts but in the opposite direction (toward

more negative potentials). The results of the stimulation are shown in Fig. 18 (top). The over-all change in diastolic interval is rather small, and in contrast to Fig. 16, the diastolic interval is *shortened* by elevating $[Ca]_o$.

Can the experimental and calculated results be reconciled? One possibility is that the shift in sodium kinetic parameters is larger than the value we have used (see Fig. 16: the 'threshold' potential shifts by 7 and 9 mV for successive fourfold increases in $[Ca]_o$). Another possible explanation is that the model parameters do not accurately represent the real separation between the voltage-dependent processes, $s$ and $m$. If, for example, the sodium parameters were located at a more negative level than that used in the reconstruction, the sodium-current-sensitive phase of the pacemaker would comprise a larger fraction of the total diastolic interval; $[Ca]_o$-dependent shifts in $m$ would thus play a larger part in determining the over-all effect. The experimental variation in location of the various parameters is rather large and makes this explanation fairly plausible. In the case of the sodium kinetics, Weidmann (1955*b*) found that the potential where $h_\infty = 0{\cdot}5$ varied between $-60$ and $-84$ mV. Similarly the 'threshold' potential for excitation by depolarizing current pulses ranged between $-60$ and $-76$ mV. A comparable degree of variability occurs in the location of the activation curve for $i_{K_2}$ (Tsien, 1974).

Fig. 18 illustrates the importance of the voltage separation between $s$ and $m$. The reconstruction of calcium-dependent shifts is repeated, but the location of the sodium current parameters in '1·8 mM calcium' has been altered to bring $s_\infty$ and $m_\infty$ closer together. In the middle and bottom panels, $\bar{E}_m$ and $\bar{E}_h$ have each been relocated by $-2{\cdot}5$ and $-5$ mV respectively, in calculating the '1·8 mM calcium' pacemaker potential. Fourfold changes in $[Ca]_o$ are modelled as in the top panel, by shifting the sodium rate coefficient curves by $+6$ mV, and $\alpha_s$ and $\beta_s$ by $+8$ mV. In the bottom panel, the results of the reconstruction now show a qualitative resemblance to the experimental results, that is, a prolongation of the diastolic interval with the 'increase in $[Ca]_o$'.

It is clear from these calculations that the overall chronotropic effect is rather sensitive to the balance between opposing changes produced by calcium ions. This is particularly apparent in the middle panel, which shows an intermediate situation where an acceleratory effect is produced by *either* an increase or a decrease in $[Ca]_o$.

## DISCUSSION

In describing the results of this paper we have already discussed some of the detailed points that arise. It remains only to draw some general conclusions, and to indicate where the model is still inadequate.

*Comparison with previous models*

Despite its limitations there can be no doubt that the present model is a considerable improvement on previous models of Purkinje fibre electrical activity. It is the first complete model to be based on the voltage clamp analyses of individual ionic current components performed over the last ten years. Although there are definite resemblances to the model described by Noble (1962*a*), the differences are very important. In Noble's model, no calcium current was included; the excitatory sodium current was given the dual function of generating the upstroke and supporting the plateau. A single time-dependent potassium current was made to perform the functions of both $i_{K_2}$ and $i_{x_1}$. The chloride current was also inadequately represented. We have already shown the ability of the new model to reproduce phenomena which were not within the scope of Noble's model. The most important of these phenomena are (*a*) the occurrence of action potentials in the absence of rapidly-activated sodium currents, (*b*) the independence of plateau and pace-maker mechanisms, and (*c*) the presence of the notch separating the spike and plateau phases of repolarization.

The present formulation also provides an advance on the partial models of pace-maker activity and repolarization described by Noble & Tsien (1968, 1969*b*). In their pace-maker model (see Fig. 13 of Noble & Tsien, 1968) the membrane potential was not a free (i.e. computed) parameter and it was not possible, therefore, to investigate the relative contributions of inward rectification and sodium activation to the diastolic depolarization. In our present effort to reconstruct pace-maker activity, we have found it necessary to revise the more rudimentary model, by emphasizing the role of sodium activation in the later stages of the pace-maker potential. This case is but one example where the reconstruction work has helped in understanding the roles of the various components in generating the overall activity. Another example is the demonstration that the outward surge of chloride current during the spike repolarization is much briefer than would be suggested by its wave form during voltage clamp steps to positive potentials (see Fig. 13).

The present equations also differ substantially from an earlier model of the repolarization process (Noble & Tsien, 1969*b*) where the activation of $i_{x_1}$ was the only important time-dependent process during the plateau. In the present reconstruction, $i_{x_1}$ activation is still viewed as the rate-limiting process in triggering the repolarization. However, $i_{si}$ (the secondary inward current, at least partly carried by calcium ions) is now incorporated, and this component allows the generation of a realistic secondary depolarization and notch configuration. The magnitude and kinetics of $i_{si}$

and $i_{x_1}$ are sensitive to experimental conditions and this may partially explain earlier controversy about the nature of the repolarization process (Reuter, 1967, 1968; Peper & Trautwein, 1968; Noble & Tsien, 1969*a*, *b*). More recent experiments (e.g. Vitek & Trautwein, 1971) and the reconstruction work leave little doubt as to the existence of both $i_{s1}$ and $i_{x_1}$ (Trautwein, 1973). In our view, both components are functionally important in normal activity as well as under the influence of adrenaline (Tsien *et al.* 1972).

By including $i_{s1}$, it has become possible to reconstruct in some detail the dynamic behaviour of the membrane in Vassalle's (1966) all-or-nothing repolarization experiments. These reconstructions have highlighted the role of the secondary inward current in the type of behaviour he observed. The importance of this component is indicated by the deep notch and long-lasting plateau phase (see Fig. 12*B*), and by the fact that hyperpolarizing pulses near threshold are followed by a temporary depolarizing response preceding the eventual repolarization (see Fig. 11*B*). The presence of substantial $i_{s1}$ is also suggested by the necessity for the potential to be clamped for as long as 20 msec at each 'threshold' potential. This was presumably the time required to deactivate $i_{s1}$ (see also Reuter, 1973). Each of these aspects of the experimental behaviour was clearly beyond the scope of Noble & Tsien's (1969*b*) reconstruction, which did not include the kinetic properties of $i_{s1}$.

### *The magnitude and location of the sodium current*

Notwithstanding the improvements made on previous models, the present reconstruction, like Noble's (1962*a*) model, suffers from a particularly important deficiency: the sodium current is inadequate to fully account for the upstroke rate and propagation velocity without making further assumptions. This problem remains despite the fact that we have included considerably more sodium current in the model than is recorded in voltage clamp experiments. Although the resolution is still unclear, we are inclined to favour the explanation that the sodium current density is not uniform throughout the preparation but is greatest in the surface cell membranes, with relatively weak currents flowing across the membranes lining the clefts between individual cells. This would allow the sodium current to discharge the surface cell membranes more rapidly and to achieve rapid propagation (see Fozzard, 1966). Thus, a peak sodium conductance similar in magnitude to that recorded experimentally (Dudel & Rüdel, 1970) is adequate to produce the observed upstroke velocity and propagation speed if it is allowed to discharge only 25% of the total capacitance (Noble, 1962*b*; see also McAllister, 1968).

However, it is difficult to see how such an uneven distribution of sodium

conductance could be detected experimentally since it is likely that the voltage clamp technique fails to record much of the sodium current occurring in cleft membranes. If the membrane conductance increase during sodium activation is of the order of 100-fold (Weidmann, 1951) then the voltage non-uniformities that would be generated in the clefts (cf. Sommer & Johnson, 1968) are certain to be very large. As a result, the voltage clamp technique would record only a small fraction of the cleft membrane sodium current. It is then difficult to distinguish this situation from one in which the cleft sodium currents are genuinely small. A comparable situation occurs in skeletal muscle where the voltage clamp currents can be shown to be relatively independent of the sodium current flowing in the transverse tubular system (Adrian & Peachey, 1973).

An uneven distribution of sodium channels would be advantageous from an energetic point of view. The function of the Purkinje fibre is to provide rapid spread of excitation throughout the ventricle and, for a given magnitude of sodium current, this is most efficiently achieved by placing the sodium conductance channels at the fibre surface.

*Use of the present model in further applications*

In presenting the equations we have used we have already emphasized an important heuristic difference between our model and that of Hodgkin & Huxley for squid nerve. Unlike the squid model, it is impossible to obtain all the required information from voltage clamp analysis of a single fibre. Moreover there is a substantial degree of natural variation between Purkinje fibres in the relative magnitudes and speeds of the different current components. Since the slow changes in potential occurring in cardiac fibres are generated by very small net currents, it is entirely possible that the magnitudes and rates that we have used in our equations will require further modification in future applications; it is clear that relatively small modifications may have a large effect on the action potential or pace-maker depolarization. Although it is tempting to determine what modifications are required to reproduce, e.g. abnormal rhythms (cf. Hauswirth, Noble & Tsien, 1969) we doubt the wisdom of exploring such modifications without also studying such phenomena experimentally. The equations described here should be helpful in determining how experimentally known changes in particular ionic currents produce their overall effects, but less appropriate as a basis for purely theoretical explorations.

Finally, it should be noted that our work relates primarily to the Purkinje fibre. The ionic currents in these fibres show quite marked differences from those in other parts of the heart and it is likely that the relative contributions of the currents to electrical activity are significantly different in atrial and ventricular fibres, where currents like $i_{K_2}$ and the

transient chloride current are not found. A model for ventricular muscle is being developed by Beeler & Reuter (see Beeler, 1971; Reuter & Beeler, 1971).

We thank Professors S. Weidmann, H. Fozzard, M. Vassalle and H. Reuter for access to unpublished records and for helpful discussions. The computations were supported by the U.S. Public Health Service Grant 5 R01 HL 13306 (National Heart and Lung Institute) and a grant from the Nova Scotia Heart Foundation. R.W.T. is an Established Investigator of the American Heart Association.

## REFERENCES

ADELMAN, W. J. & TAYLOR, R. E. (1961). Leakage current rectification in the squid giant axon. *Nature, Lond.* **190**, 883–885.

ADRIAN, R. H. & PEACHEY, L. D. (1973). Reconstruction of the action potential of frog sartorius muscle. *J. Physiol.* **235**, 103–131.

ADRIAN, R. H. (1969). Rectification in muscle membrane. *Prog. Biophys. molec. Biol.* **19**, 341–369.

ADRIAN, R. H., CHANDLER, W. K. & HODGKIN, A. L. (1970). Voltage clamp experiments in striated muscle fibres. *J. Physiol.* **208**, 607–644.

ARONSON, R. S. & CRANEFIELD, P. F. (1973). The electrical activity of canine Purkinje fibres in sodium-free, calcium-rich solutions. *J. gen. Physiol.* **61**, 786–808.

BEELER, G. W. (1971). Numerical reconstruction of the myocardial action potential. *Proc. int. Union Physiol. Sci. Munich*, p. 48.

BEELER, G. W. & REUTER, H. (1970). Voltage clamp experiments on ventricular myocardial fibres. *J. Physiol.* **207**, 165–190.

BOSTEELS, S. & CARMELIET, E. (1972). Estimation of intracellular sodium concentration and transmembrane sodium flux in cardiac Purkinje fibres. *Pflügers Arch. ges. Physiol.* **376**, 35–47.

BOSTEELS, S., VLEUGELS, A. & CARMELIET, E. (1970). Choline permeability in cardiac muscle cells of the cat. *J. gen. Physiol.* **55**, 602–619.

BOULPAEP, E. (1963). Permeability of heart muscle to choline. *Archs int. Physiol.* **71**, 623–625.

BRADY, A. J. & WOODBURY, J. W. (1960). The sodium-potassium hypothesis as the basis of electrical activity in frog ventricle. *J. Physiol.* **154**, 385–407.

CARMELIET, E. (1961). Chloride ions and the membrane potential of Purkinje fibres. *J. Physiol.* **156**, 375–388.

CARMELIET, E. & VEREECKE, J. (1969). Adrenaline and the plateau phase of the cardiac action potential. *Pflügers Arch. ges. Physiol.* **313**, 303–315.

CRANEFIELD, P. F. & HOFFMAN, B. F. (1958). Propagated repolarization in heart muscle. *J. gen. Physiol.* **41**, 633–649.

CRANEFIELD, P. F., WIT, A. L. & HOFFMAN, B. F. (1972). Conduction of the cardiac impulse. III. Characteristics of very slow conduction. *J. gen. Physiol.* **59**, 227–246.

DECK, K. A., KERN, R. & TRAUTWEIN, W. (1964). Voltage clamp technique in mammalian cardiac fibres. *Pflügers Arch. ges. Physiol.* **280**, 50–62.

DECK, K. A. & TRAUTWEIN, W. (1964). Ionic currents in cardiac excitation. *Pflügers Arch. ges. Physiol.* **280**, 65–80.

DODGE, F. A. & FRANKENHAEUSER, B. (1958). Membrane currents in isolated frog nerve fibre under voltage clamp conditions. *J. Physiol.* **143**, 76–90.

DRAPER, M. H. & WEIDMANN, S. (1951). Cardiac resting and action potentials recorded with an intracellular electrode. *J. Physiol.* **115**, 74–94.

DUDEL, J., PEPER, K., RÜDEL, R. & TRAUTWEIN, W. (1966). Excitatory membrane current in heart muscle (Purkinje fibres). *Pflügers Arch. ges. Physiol.* **192**, 255–273.

DUDEL, J., PEPER, K., RÜDEL, R. & TRAUTWEIN, W. (1967*a*). The dynamic chloride component of membrane current in Purkinje fibres. *Pflügers Arch. ges. Physiol.* **195**, 197–212.

DUDEL, J., PEPER, K., RÜDEL, R. & TRAUTWEIN, W. (1967*b*). The effect of tetrodotoxin on the membrane current in cardiac muscle (Purkinje fibres). *Pflügers Arch. ges. Physiol.* **295**, 213–226.

DUDEL, J., PEPER, K., RÜDEL, R. & TRAUTWEIN, W. (1967*c*). The potassium component of membrane current in Purkinje fibres. *Pflügers Arch. ges. Physiol.* **296**, 308–327.

DUDEL, J. & RÜDEL, R. (1970). Voltage and time dependence of excitatory sodium current in cooled sheep Purkinje fibres. *Pflügers Arch. ges. Physiol.* **315**, 136–158.

FITZHUGH, R. (1960). Thresholds and plateaus in the Hodgkin–Huxley nerve equations. *J. gen. Physiol.* **43**, 867–896.

FOZZARD, H. A. (1966). Membrane capacity of the cardiac Purkinje fibre. *J. Physiol.* **182**, 255–267.

FOZZARD, H. A. & GIBBONS, W. R. (1973). Action potential and contraction of heart muscle. *Am. J. Cardiol.* **31**, 182–192.

FOZZARD, H. A. & HIRAOKA, M. (1973). The positive dynamic current and its inactivation properties in cardiac Purkinje fibres. *J. Physiol.* **234**, 569–586.

FOZZARD, H. A. & SCHOENBERG, M. (1972). Strength-duration curves in cardiac Purkinje fibres: effects of liminal length and charge redistribution. *J. Physiol.* **226**, 593–618.

FRANKENHAEUSER, B. & PERSSON, A. (1957). Voltage clamp experiments on the myelinated nerve fibre. *Acta physiol. scand.* **42**, suppl. 145.

FREYGANG, W. H. & TRAUTWEIN, W. (1970). The structural implications of the linear electrical properties of cardiac Purkinje fibres. *J. gen. Physiol.* **55**, 524–547.

GETTES, L., MOREHOUSE, N. & SURAWICZ, B. (1972). Effect of premature depolarization on action potential duration in Purkinje and ventricular fibres of the pig moderator band. Role of preceding action potential duration and proximity. *Circulation Res.* **30**, 55–66.

GEORGE, E. P. & JOHNSON, E. A. (1961). Solutions of the Hodgkin-Huxley equations for squid axon treated with tetraethylammonium ion and in potassium rich media. *Aust. J. exp. Biol. med. Sci.* **39**, 275–293.

HAAS, H. G. & KERN, R. (1966). Potassium fluxes in voltage clamped Purkinje fibres. *Pflügers Arch. ges. Physiol.* **291**, 69–84.

HALL, A. E., HUTTER, O. F. & NOBLE, D. (1963). Current–voltage relations of Purkinje fibres in sodium-deficient solutions. *J. Physiol.* **166**, 225–240.

HALL, A. E. & NOBLE, D. (1963). Transient responses of Purkinje fibres to non-uniform currents. *Nature, Lond.* **199**, 1294–1295.

HAUSWIRTH, O. (1971). Computer-Rekonstructionen der Effekte von Polarisationsströmen und Pharmaka auf Schrittmacher- und Aktionspotentiale von Herzmuskelfasern. Habilitationsschrift, University of Heidelberg.

HAUSWIRTH, O., MCALLISTER, R. E., NOBLE, D. & TSIEN, R. W. (1968). Measurement of voltage clamp currents and reconstruction of electrical activity in Purkinje fibres under normal conditions and under the influence of adrenaline. *J. Physiol.* **198**, 8–10*P*.

HAUSWIRTH, O., MCALLISTER, R. E., NOBLE, D. & TSIEN, R. W. (1969). Reconstruction of the actions of adrenaline and calcium on cardiac pacemaker potentials. *J. Physiol.* **204**, 126–128*P*.

HAUSWIRTH, O., NOBLE, D. & TSIEN, R. W. (1968). Adrenaline: mechanism of action on the pacemaker potential in cardiac Purkinje fibres. *Science, N.Y.* **162**, 916–917.

HAUSWIRTH, O., NOBLE, D. & TSIEN, R. W. (1969). The mechanism of oscillatory activity at low membrane potentials in cardiac Purkinje fibres. *J. Physiol.* **200**, 255–265.

HAUSWIRTH, O., NOBLE, D. & TSIEN, R. W. (1972*a*). The dependence of plateau currents in cardiac Purkinje fibres on the interval between action potentials. *J. Physiol.* **222**, 27–49.

HAUSWIRTH, O., NOBLE, D. & TSIEN, R. W. (1972*b*). Separation of the pace-maker and plateau components of delayed rectification in cardiac Purkinje fibres. *J. Physiol.* **225**, 211–235.

HECHT, H. H., HUTTER, O. F. & LYWOOD, D. W. (1964). Voltage-current relation of short Purkinje fibres in sodium-deficient solution. *J. Physiol.* **170**, 5–6*P*.

HILLE, B. (1970). Ionic channels in nerve membranes. *Prog. Biophys. molec. Biol.* **21**, 1–32.

HODGKIN, A. L. (1951). The ionic basis of electrical activity in nerve and muscle. *Biol. Rev.* **26**, 339–409.

HODGKIN, A. L. & HUXLEY, A. F. (1952). A quantitative description of membrane current and its application to conduction and excitation in nerve. *J. Physiol.* **117**, 500–544.

HUTTER, O. F. & NOBLE, D. (1960). Rectifying properties of heart muscle. *Nature, Lond.* **188**, 495.

HUTTER, O. F. & NOBLE, D. (1961). The anion conductance of cardiac muscle. *J. Physiol.* **157**, 335–350.

JOHNSON, E. A. & LIEBERMAN, M. (1971). Heart: excitation and contraction. *A. Rev. Physiol.* **33**, 479–532.

MCALLISTER, R. E. (1968). Computed action potentials for Purkinje fibre membrane with resistance and capacitance in series. *Biophys. J.* **8**, 951–964.

MCALLISTER, R. E. (1970). Two programs for computation of action potentials, stimulus response, voltage-clamp currents, and current-voltage relations of excitable membranes. *Computer Programs in Biomedicine*, **1**, 146–166.

MCALLISTER, R. E. & NOBLE, D. (1966). The time and voltage dependence of the slow outward current in cardiac Purkinje fibres. *J. Physiol.* **186**, 632–662.

MCALLISTER, R. E. & NOBLE, D. (1967). The effect of subthreshold potentials on the membrane current in cardiac Purkinje fibres. *J. Physiol.* **190**, 381–387.

MOBLEY, B. A. & PAGE, E. (1972). The surface area of sheep cardiac Purkinje fibres. *J. Physiol.* **220**, 547–563.

MOORE, J. W. & RAMON, F. (1974). On numerical integration of the Hodgkin and Huxley equations for a membrane action potential. *J. theor. Biol.* **45**, 249–273.

NEW, W. & TRAUTWEIN, W. (1972). Inward membrane currents in mammalian myocardium. *Pflügers Arch. ges. Physiol.* **334**, 1–23.

NOBLE, D. (1960). Cardiac action and pacemaker potentials based on the Hodgkin–Huxley equations. *Nature, Lond.* **188**, 495–497.

NOBLE, D. (1962*a*). A modification of the Hodgkin–Huxley equations applicable to Purkinje fibre action and pacemaker potentials. *J. Physiol.* **160**, 317–352.

NOBLE, D. (1962*b*). Computed action potentials and their experimental basis. *Proc. int. Union Physiol. Sci.* **1**, 177–182.

NOBLE, D. (1972*a*). Conductance mechanisms in excitable cells. *Biomembranes* **3**, 427–447.

NOBLE, D. (1972*b*). The relation of Rushton's 'liminal length' for excitation to the resting and active conductances of excitable cells. *J. Physiol.* **226**, 573–591.

NOBLE, D. (1974). Cardiac action potentials and pace-maker activity. *Recent Advances in Physiology*, ed. LINDEN, R. J., pp. 1–50. London: Churchill.

NOBLE, D. & HALL, A. E. (1963). The conditions for initiating 'all-or-nothing' repolarization in cardiac muscle. *Biophys. J.* **3**, 261–274.

NOBLE, D. & TSIEN, R. W. (1968). The kinetics and rectifier properties of the slow potassium current in cardiac Purkinje fibres. *J. Physiol.* **195**, 185–214.

NOBLE, D. & TSIEN, R. W. (1969*a*). Outward membrane currents activated in the plateau range of potentials in cardiac Purkinje fibres. *J. Physiol.* **200**, 205–231.

NOBLE, D. & TSIEN, R. W. (1969*b*). Reconstruction of the repolarization process in cardiac Purkinje fibres based on voltage clamp measurements of the membrane current. *J. Physiol.* **200**, 233–254.

NOBLE, D. & TSIEN, R.W. (1972). The repolarization process of heart cells. In *Electrical Phenomena in the Heart*, ed. DE MELLO, W. C., pp. 133–161. New York: Academic Press.

OTSUKA, M. (1958). Die Wirkung von Adrenalin auf Purkinje-Fasern von Säugetierherzen. *Pflügers Arch. ges. Physiol.* **266**, 512–517.

PEPER, K. & TRAUTWEIN, W. (1968). A membrane current related to the plateau of the action potential of Purkinje fibres. *Pflügers Arch. ges. Physiol.* **303**, 108–123.

PEPER, K. & TRAUTWEIN, W. (1969). A note on the pacemaker current in Purkinje fibres. *Pflügers Arch. ges. Physiol.* **309**, 356–361.

REUTER, H. (1967). The dependence of the slow inward current on external calcium concentration in Purkinje fibres. *J. Physiol.* **192**, 479–492.

REUTER, H. (1968). Slow inactivation of currents in cardiac Purkinje fibres. *J. Physiol.* **197**, 233–253.

REUTER, H. (1973). Divalent cations as charge carriers in excitable membranes. *Prog. Biophys. molec. Biol.* **26**, 1–43.

REUTER, H. & BEELER, G. W. (1971). The mechanism of all-or-nothing repolarization in ventricular myocardial fibres. *Proc. int. Union Physiol. Sci.* 472.

ROUGIER, O., VASSORT, G., GARNIER, D., GARGOUIL, Y-M., & CORABOEUF, E. (1969). Existence and role of a slow inward current during the frog atrial action potential. *Pflügers Arch. ges. Physiol.* **308**, 91–110.

SOMMER, J. R. & JOHNSON, E. A. (1968). Cardiac muscle: a comparative study of Purkinje fibres and ventricular fibres. *J. cell Biol.* **36**, 497–526.

TEMTE, J. & DAVIS, L. (1967). Effect of calcium concentration on the transmembrane potential of Purkinje fibres. *Circulation Res.* **20**, 32–44.

TRAUTWEIN, W. (1973). Membrane currents in cardiac muscle fibres. *Physiol. Rev.* **53**, 793–835.

TRAUTWEIN, W. & SCHMIDT, R. F. (1960). Membranwirkung des Adrenalins an der Herzmuskelfaser. *Pflügers Arch. ges. Physiol.* **271**, 715–726.

TSIEN, R. W. (1974). Effects of epinephrine on the pace-maker potassium current of cardiac Purkinje fibres. *J. gen. Physiol.* **64**, 293–319.

TSIEN, R. W., GILES, W. R. & GREENGARD, P. (1972). Cyclic AMP mediates the action of adrenaline on the action potential plateau of cardiac Purkinje fibres. *Nature, New Biol.* **240**, 181–183.

VASSALLE, M. (1966). Analysis of cardiac pace-maker potential using a 'voltage clamp' technique. *Am. J. Physiol.* **210**, 1335–1341.

VASSALLE, M. (1970). Electrogenic suppression of automaticity in sheep and dog Purkinje fibres. *Circulation Res.* **27**, 361–377.

VASSALLE, M. & BARNABEI, O. (1971). Norepinephrine and potassium fluxes in cardiac Purkinje fibres. *Pflügers Arch. ges. Physiol.* **322**, 287–303.

VITEK, M. & TRAUTWEIN, W. (1971). Slow inward current and action potentials in cardiac Purkinje fibres. *Pflügers Arch. ges. Physiol.* **323**, 204–218.

WEIDMANN, S. (1951). Effect of current flow on the membrane potential of cardiac muscle. *J. Physiol.* **115**, 227–236.

WEIDMANN, S. (1952). The electrical constants of Purkinje fibres. *J. Physiol.* **118**, 348–360.

WEIDMANN, S. (1955*a*). The effect of the cardiac membrane potential on the rapid availability of the sodium carrying system. *J. Physiol.* **127**, 213–224.

WEIDMANN, S. (1955*b*). Effects of calcium ions and local anaesthetics on electrical properties of Purkinje fibres. *J. Physiol.* **129**, 568–582.

WEIDMANN, S. (1956). *Elektrophysiologie der Herzmuskelfaser*. Bern: Huber.

WEIDMANN, S. (1964). Allgemeine Elektrophysiologie bei Stillstand und Wiedereinsetzen der Herztätigkeit. *Verh. ges. dt. Naturf. Arzte* **30**, 1–10.